Palaeontologia Electronica
palaeo-electronica.org

Were terror birds the apex continental predators of Antarctica? New findings in the early Eocene of Seymour Island

Carolina Acosta Hospitaleche and Washington Jones

ABSTRACT

Two ungual phalanges attributed to large birds were collected in the Ypresian (early Eocene) levels of the Cucullaea Allomember (Submeseta Formation). Both materials were found in localities in proximity on Seymour Island in West Antarctica. The pronounced curvature, considerable size robustness, and the extension of the flexor tubercle provide compelling evidence for their classification within Cariamiformes. Additionally, the results of quantitative analyses strongly support this assignment to Phorusrhacidae or a Phorusrhacidae-like bird resembling *Phorusrhacos longissimus.* These phalanges belonged to a large or even giant predator, estimated to have had a substantial body mass of around 100 kg. It is highly likely that this bird was an active predator, hunting and feeding on small marsupials and medium-sized ungulates. This finding fundamentally changes our understanding of the dynamic within the Antarctic continental ecosystems during the early Eocene. It reveals that large carnivorous birds assumed the role of continental apex predators apparently sub-occupied by mammals.

Carolina Acosta Hospitaleche. División Paleontología de Vertebrados, Museo de La Plata. Paseo del Bosque s/n B1900FWA, La Plata, Facultad de Ciencias Naturales y Museo, Universidad Nacional de La Plata, Argentina and CONICET, Godoy Cruz 2290, Ciudad Autónoma de Buenos Aires, Argentina. acostacaro@fcnym.unlp.edu.ar
Washington Jones. Museo Nacional de Historia Natural. 25 de mayo 582 P.C. 11000. Montevideo, Uruguay. wawijo78@gmail.com

Keywords: ungual phalanx, anatomy, Cariamiformes, Phorusrhacidae, Antarctic Peninsula, Ypresian

Submission: 13 September 2023. Acceptance: 10 November 2023.

INTRODUCTION

Cariamiformes is an order of mainly terrestrial birds that exhibits a significant past diversification but only two species are living today in South America. Despite the rich fossil record, the phylogenetic and biogeographic relationships within this order remain poorly understood. Within the Cari-

Final citation: Acosta Hospitaleche, Carolina and Jones, Washington. 2024. Were terror birds the apex continental predators of Antarctica? New findings in the early Eocene of Seymour Island. Palaeontologia Electronica, 27(1):a13.
https://doi.org/10.26879/1340
palaeo-electronica.org/content/2024/5162-eocene-cariamiformes-from-antarctica

amiformes, Phorusrhacidae composes the crown-group with Cariamidae, while Idiornithidae and Bathornthidae have been identified recoveredidentified as fossil families. However, affinities of other putative cariamiforms and cariamiform-like birds are still unresolved (Mayr, 2016a, 2022). The crown-group Cariamidae-Phorusrhacidae is well supported (Degrange, 2012; Mayr, 2016a) and has also been widely recognized in the past (Brodkorb, 1967; Cracraft, 1968, 1971; Mourer-Chauviré, 1983; Alvarenga and Höfling, 2003; Alvarenga et al., 2011). In one of the most comprehensive analyses, several characters specifically identified on the phalanges, such as a notably short proximal phalanx in the first toe, an abbreviated proximal phalanx of second toe, and the penultimate phalanx of four toe, a strongly curved and sharply hooked ungual phalanx of the second toe, and the absence of sulcus neurovascularis in all the ungual phalanges, were proposed as synapomorphies for this clade (Mayr, 2016a).

Cariamidae consists of the two extant species, both endemic to South America: *Chunga burmeisteri* and *Cariama cristata* (Gonzaga, 1992; Winkler et al., 2020). Additionally, it includes the extinct *Chunga incerta* from the early Pliocene Monte Hermoso Formation and *Miocariama patagonica* from the early Miocene Santa Cruz Formation (Tonni, 1974; Noriega and Mayr, 2017). Other records involve uncertain specimens, such as the tarsometatarsus from the early Miocene Santa Cruz Formation in the Magallanes Region, Chile (Soto-Acuña et al., 2014).

The completely extinct Phorusrhacidae, commonly known as “terror birds”, includes the Psilopterinae, Mesembriornithinae, “Physornithinae”, “Phorusrhacinae”“, and “Patagornithinae”. Brontornithinae was classically considered a phorusrhacid (Moreno and Mercerat, 1891; Alvarenga et al., 2011; Alvarenga and Höfling, 2003; Mayr, 2022), then suggested to be more closely related to Anseriformes (Agnolín, 2009; Degrange et al., 2015), and subsequently repositioned within Neoaves, close to Cariamiformes (Worthy et al., 2017; see however Agnolín, 2021).

One of the earliest records of putative Phorusrhacidae corresponds to the Eocene *Paleopsilopterus itaboraiensis* (Alvarenga, 1985; Alvarenga and Höfling, 2003). This species is represented by a proximal end of tarsometatarsus and two distal ends of tibiotarsus (Alvarenga, 1985). Initially, it was classified in Psilopterinae, but later reevaluated and placed in Idiornithidae (Agnolín, 2009), and alternatively as iIndeterminant family within Cariamiformes (Degrange, 2012). Subsequently, it was placed into Phorusrhacidae Psilopterinae (Tambussi and Degrange, 2013) and then into Idiornithidae (Tambussi et al., 2023). In addition, a fragmentary tarsometatarsus and an ungual phalanx from the late Eocene of Gran Hondonada (Acosta Hospitaleche and Tambussi, 2005; age updated according to Kramarz et al., 2019) were assigned to a Psilopterinae. Although these remains were assigned to undetermined species, Agnolín (2009) identified it as a new genus and species of Idiornithidae. Alternatively, these remains were considered as Cariamiformes indet. (Degrange, 2012), but then treated as Idiornithidae (Tambussi et al., 2023). Therefore, the oldest and non-controversial record would correspond to a single distal end of tibiotarsus from the middle Eocene of Cañadón Vaca (Tonni and Tambussi, 1986; age updated according to Dunn et al., 2015).

Phorusrhacidae have therefore been documented, at least, from the middle Eocene, and were predominantly found in South America, persisting until the Pleistocene (Jones et al., 2018). However, during the Pliocene, Phorusrhacidae expanded its range to North America during the Great American Biotic Interchange (Brodkorb, 1963; McFadden et al., 2007). African and European records (Mourer-Chauviré et al., 2011; Angst et al., 2013; Angst and Buffettaut, 2017; Buffetaut and Angst, 2021) have been the subject of controversy. They may be related cariamiforms (Mayr, 2016a), although some authors considered them members of Phorusrhacidae (Tambussi et al., 2023). This ongoing debate underscores the need for further research and analysis to clarify the taxonomic affiliations of these specimens.

After the finding of two ungual phalanges in the Eocene of Antarctica that bear a striking resemblance to Phorusrhacidae, previous mentions of these groups were reevaluated. Four isolated Antarctic elements have been previously identified as Phorusrhacidae (Case et al., 1987, 2006; Tambussi and Noriega, 1996; Chavez, 2007; Tambussi and Acosta Hospitaleche, 2007). The first one is a premaxillary fragment (UCR 22175) from the Eocene Submeseta Formation (La Meseta Formation in Case et al., 1987), that was re-considered ratites (Cenizo, 2012) and, almost simultaneously, considered morphologically similar to Pelagornithidae (Tambussi and Degrange, 2013). Subsequently, other fossils were assigned to, or associated with, terror birds, including a left femur from the Maastrichtian (López de Bertodano Formation) of Vega Island (Case et al., 2006),

which was recently identified as *Vegavis* (West et al., 2019). Also, a tibiotarsus and a cervical vertebra from the Submeseta Formation that were questioned in Tambussi and Acosta Hospitaleche (2007) and dismissed in posterior contributions. Finally, the distal end of a right tarsometatarsus (UCR 22176) was later placed within Pelagornithidae (Cenizo, 2012). Additionally, several ichnites were discovered in the middle Eocene deposits of the Fossil Hill Formation, in the homonymous locality of Fildes Peninsula, in King George Island, South Shetland Islands (West Antarctica). Among these, two poorly preserved avian tracks referred to ‘‘Morphotype I’’ were assigned either to ratites or phororhacoid birds (Covacevich and Rich, 1982; Mansilla et al., 2012a).

In summary, over the past decade, all the Cretaceous and Paleogene Antarctic remains previously referred to Phorusrhacidae have been reassigned to other groups. Nevertheless, the two ungual phalanges recently found in Ypresian levels of La Meseta Formation from the Marambio/Seymour Island (James Ross Basin), can be unequivocally assigned to Cariamiformes, specifically to a Phorusrhacidae-like bird. The primary objective of the present contribution is to analyze these phalanges in detail.

GEOLOGICAL SETTING

The materials under examination come from Seymour/Marambio Island (Figure 1A-C), a small landmass located to the east of the Antarctic Peninsula and near its northern end (Figure 1C). This island, characterized by a fossil rich uppermost sequence, remains devoid of ice cover during the austral summer, enabling the extensive exposure of Cretaceous-Paleogene outcrops (see Montes et al. 2013, 2019).

The stratigraphic sequence comprises the early Maastrichtian- Danian Marambio Group (Rinaldi et al., 1978), and the overlying Seymour Island Group (Zinsmeister, 1982) (Figure 1C). The latter comprises the Selandian-Thanetian Cross Valley-Wiman Formation (Montes et al., 2008a, b), the Thanetian-Lutetian La Meseta Formation (Rinaldi et al., 1978; Marenssi et al., 1998), and the Lutetian-Priabonian-Rupelian? Submeseta Formation, which represents the last stage of basin clogging (Montes et al., 2019). The La Meseta Formation (sensu Montes et al., 2013, 2019; but see also Marenssi et al., 1998, which included the current Submeseta Formation as its uppermost allomember), is internally divided into six allomembers (Figure 1B) named Valle de las Focas, Acantilados I, Acantilados II, Campamento, Cucullaea I, and Cucullaea II, from base to top (Montes et al., 2019).

The Cucullaea I (=Cucullae) Allomember presents a stratigraphicallystratigraphic structure, comprising two distinguishable internal terms. The lower term is characterized by rhythmic alternation of silts and sands with two densely packed beds (35Cu1 and 35Cu2). These beds are dominated by the bivalve *Cucullaea raea* and scarce bioturbation restricted to the muddy intervals. The upper term becomes sandier, more bioturbated, and contains a coquina level (35n) almost exclusively composed of the gastropod *Natica* sp.

Above, another two levels with densely packed shells (35Cu3 and 35Cu4) composed of *Cuccullae* sp. are identified and these can be followed relatively continuously in each of the localities (Montes et al., 2019). Both specimens MLP-PV 13-XI-28-546 and MLP-PV 14-I-10-199 come from levels deposited above 35n (Figure 1A-B).

MLP-PV 13-XI-28-546 was collected in the locality IAA 2/13, (informally known as “Simil RV”, Figure 1A-B) due to its stratigraphic correlation with the locality DPV 6/84 or RV 8200 in Woodburne and Zinsmeister (1984). The holotype of the smallest penguin species *Aprosdokitos microtero* comes also from there (Acosta Hospitaleche et al., 2017), together with other penguin bones and abundant invertebrates. The second phalanx, MLP-PV 14-I-10-199 was found in nearby equivalent levels (Figure 1A) characterized by abundant starfish, non-bioturbated trunks, and a turtle carapace plate. The holotype of the starfish species *Zoroaster marambioensis,* along with an extensive and exceptionally well-preserved bed of asteroid specimens in their life position, come from the same locality (Palópolo et al., 2021).

MATERIAL AND METHODS

Materials. The fossils described in this contribution are permanently housed in the collections of the Vertebrate Paleontology Department of the Museo de La Plata (MLP), La Plata (Argentina). Comparative materials consist of ungual phalanges without their keratinous sheats from both extant and extinct species, sourced from various collections: Ornithological section of the Vertebrate Zoology (MLP-O) and Vertebrate Paleontology Departments (MLP-PV) of the Museo de La Plata (Argentina), Ornithological and Vertebrate Paleontology (MACN-Pv and MACN-A) Sections of the Museo Argentino de Ciencias Naturales Bernardino Rivadavia (MACN) of Ciudad Autónoma de Buenos Aires (Argentina),

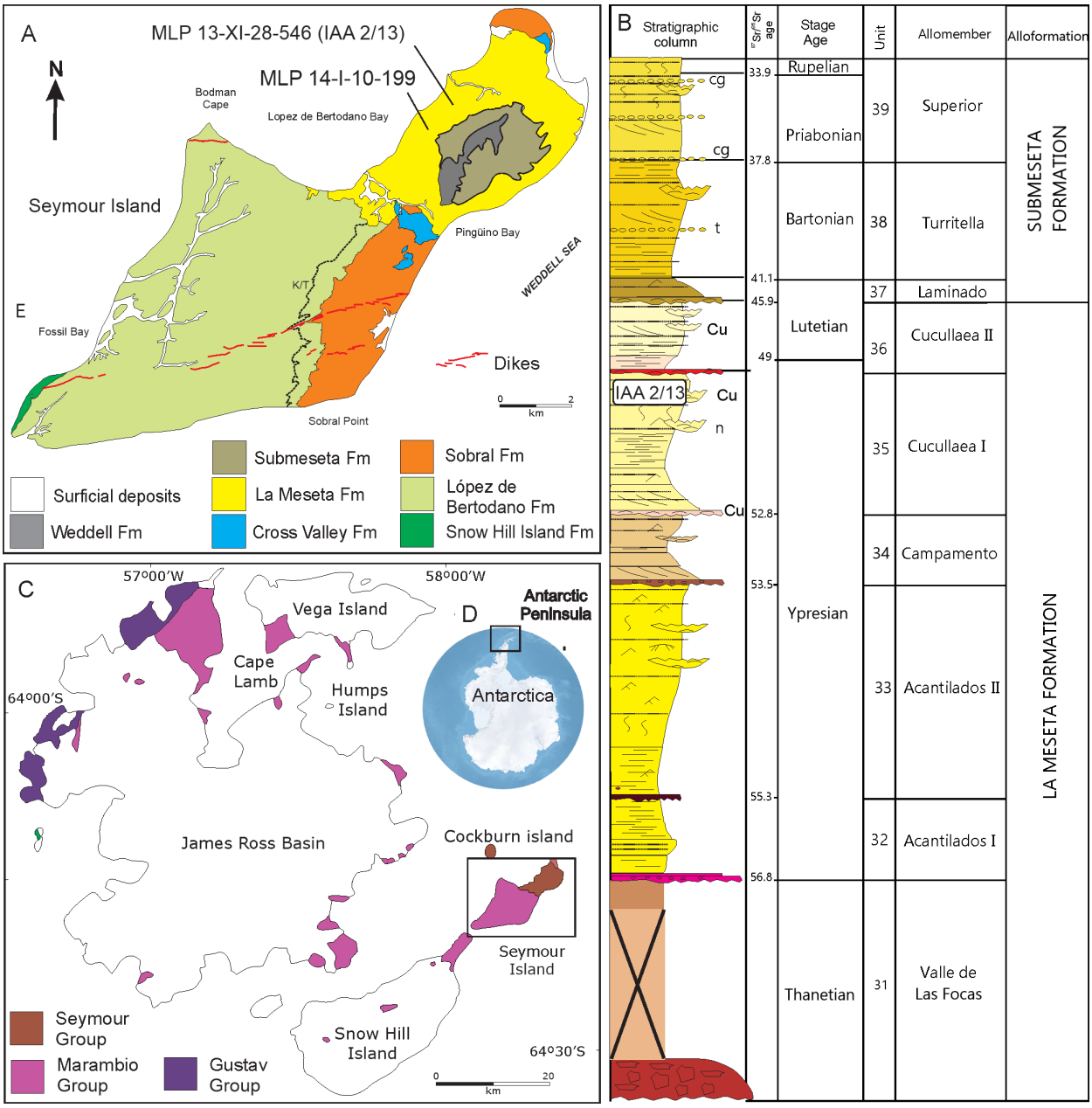

FIGURE 1. Geological map of the Seymour Island showing the fossiliferous sites where MLP-PV 13-XI-28-546 and MLP-PV 14-I-10-199 were found (A) and the corresponding stratigraphy of the locality IAA 2/13 (B), in the James Ross Basin (C), West Antarctica (D). Modified from Montes et al. (2019).

Museo Paleontológico Egidio Feruglio (MPEF-Pv), Trelew (Argentina); Museo Municipal de Ciencias Naturales Lorenzo Scaglia (MMP), Mar del Plata (Argentina), Museo de Historia Natural de la Universidad Nacional Mayor de San Marcos (MUSM), Lima (Peru), Museu de Historia Natural de Taubaté (MHNT), Taubaté (Brazil), Museo Nacional de Historia Natural (MNHN), Montevideo (Uruguay), Canterbury Museum (CMC-Av), Christchurch (New Zealand), University of California (UCR), Riverside (USA); University of Florida (UF), Gainesville (USA) (Appendix 1). Descriptions follow the terminology proposed by Baumel et al. (1993) using the English equivalent terms (Figure 2).

Data survey. Qualitative and quantitative characters, photographs, and drawings for descriptions and analyses were taken by the authors. A Caliper Vernier of 0.01 mm of increment was used for linear measurements (modified from Jones, 2010), and a degrees-scale protractor for the angular ones (Table 1). Among the qualitative features,

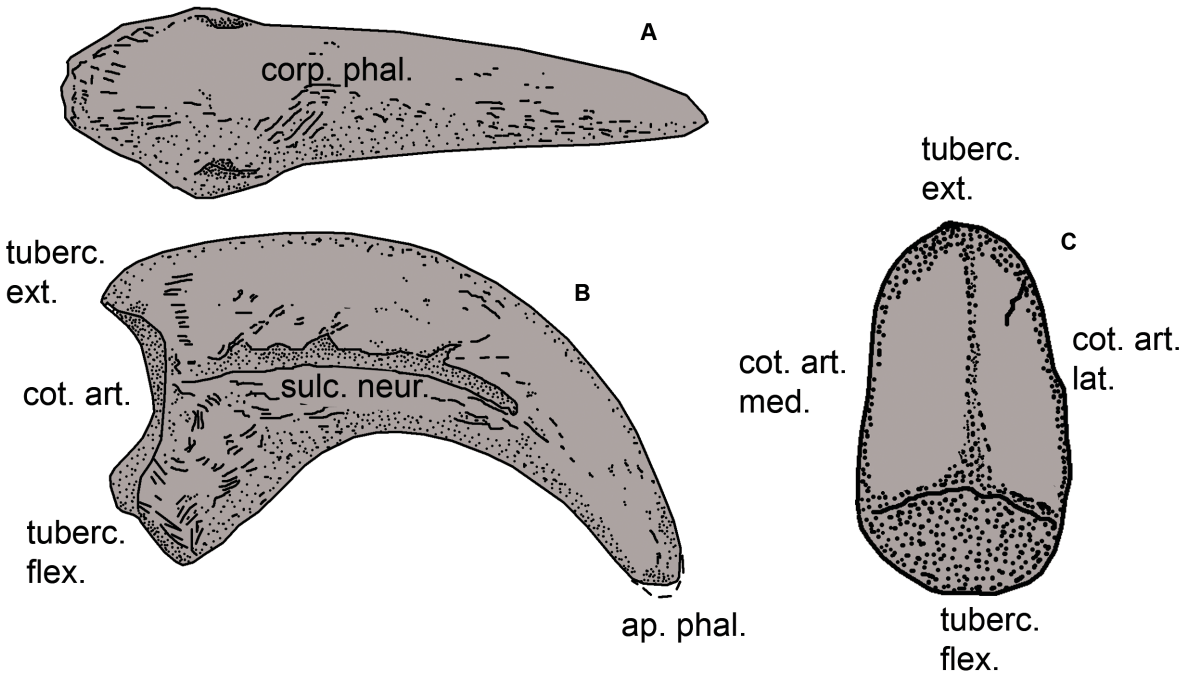

FIGURE 2. Anatomical terms used for descriptions and comparisons (after Baumel et al., 1993) in A, dorsal; B, lateral; and C, proximal views. Abbreviations: ap. phal., apex phalanx; corp. phal., corpus phalangis; cot. art., cotyla articularis (articular or proximal face); cot. art. lat., cotyla articularis lateralis; cot. art. med., cotyla articularis medialis; sulc. neur., sulcus neurovascularis (neurovascular sulcus); tuberc. ext., tuberculum extensorium (extensor tubercle); tuberc. flex., tuberculum flexorium (flexor tubercle).

which were predominantly observed with the naked eye and a binocular microscope Arcano ZTX Zoom (10-40X), particular attention was devoted to the detailed assessment of the structure of the sulcus neurovascularis. This feature was extensively examined due to its frequent utilization as a diagnostic character and its inclusion in modern phylogenetic analyses. To determine if the absence of a sulcus implied the necessary presence of a more internal canal (not externally visible), three-dimensional images were acquired using two different tomographs from the Rayodent Integral Center of Dental Radiology from La Plata, Argentina (Table 2).

The quantitative variables employed in this study were selected based on the outcomes of previous analyses (Jones, 2010). Linear measurements (Figure 3, Table 1, and Supplementary Material) were taken in millimeters and refer to the total length (TL), maximum height of the articular facet (HAF), maximum width of articular facet (WAF), flexor tubercle length (LFT), and basal height (BH) of the ungual phalanges of digit II.

To represent the curvature of the corpus phalanx, we assessed three different measurements: the outer curvature (Pike and Maitland, 2004), the inner curvature (Feduccia, 1993), and the radius and angle of curvature (Mosto and Tambussi, 2014). We noted that the inner curvature (Figure 3B), originally proposed to determine the habit of *Archaeopteryx* (Feduccia, 1993), incorporated a significant amount of error during the manual drawing of the internal arch for subsequent measurement (also noticed by Birn-Jeffery et al., 2012). It was not clear for us the mode in which the chord AB (Feduccia, 1993: fig. 1) should be objectively traced in our material to represent the inner angle, especially considering the absence of the horny sheath and the soft tissues covering the entire digit. Due to these difficulties in measurement, we decided not to include the inner curvature in the quantitative analyses. However, we did trace it for calculation of the robusticity index (see below). It is worth noting that these difficulties might have been caused by the unique morphology of the ungual phalanges of predatory and raptorial birds, which were intentionally excluded in the analysis of Feduccia (1993). The outer curvature, according to the proposal of Pike and Maitland (2004) was freehand traced (Figure 3A) for each claw. A line from the

TABLE 1. Measurements (in millimeters) taken, and indices calculated in the ungual phalanges (digit II) of the Cariamiformes specimens included in the PCA.

Material	Taxon	Total length (TL)	Inner angle (degrees)	Outer angle (degrees)	Flexor tubercule length (LFT)	Basal heigth (BH)	HAF/WAF	Robusticity index
MLP-PV 23-22 I-9	**?**Phorusrhacidae indet.	62.1*	115	117	10.3	21	1.07	0.41
MACN 6681	*Devincenzia pozzi*	67.2*	132	125	17.7	34.2	1.39	0.46
UF10417	*Titanis walleri*	79.5*	110	121	15.5	45	1.19	0.36
DGM-1418-R	*Paraphysornis brasiliensis*	77.3*	99	93	19.5	29	1.74	0.41
MLP-PV 59-II-26-82-83	*Andrewsornis abbotti*	43.8*	103	115	11.4	16	1.53	0.41
AMNH 9497	*Phorusrhacos longissimus*	62.5*	124	124	11.6	23.6	1.19	0.41
MLP-PV 76 –IV-12-2	*Psilopterus colzecus*	26*	130	116	6.6	9.4	1.74	0.45
MACN 8275	*Procariama simplex*	25.4*	115	109	4.6	9	1.72	0.46
#	*Cariama cristata*	17	143	120	3.4	6.5	1.31	0.48
MLP ORN 629	*Chunga burmeisteri*	11.8	105	92	2.8	4.4	1.25	0.44

Estimated measure.
#Mean measurements (N=3).

proximalmost point (A) to the tip (B) was drawn. The chord AB was bisected by the perpendicular CD, locating point C on the outer curvature of the phalanx. Subsequently, lines AC and BC were traced, enabling the drawing of two perpendicular lines bisecting them. The intersection of these perpendiculars, when traced toward the center of the circle, determines the point to trace the radii (RC) connecting AO and BO. The outer curvature angle was measured in degrees, from the angle subtended between both radii, and then converted into radians (Table1). Finally, the radius and angle of curvature, as used by Mosto and Tambussi (2014: fig. 1) to analyze the phalanges of diurnal birds of prey, were essentially modifications of the measurements proposed by Pike and Maitland (2004). After evaluating these variables, we decided to exclude them to prevent redundant information (see Appendix 2 for further details).

The relative robusticity was computed in accordance with the method described by Birn-Jeffery et al (2012), which begins with the inner curvature angle *sensu* Feduccia (1993). The chord AB was traced connecting the base and tip of the phalanx. Then, the perpendicular line CD was drawn at the midpoint (C) of AB, with point D located on the outer (dorsal) curvature and D' on the inner (plantar) curvature of the phalanx. The robusticity index was calculated as the ratio DD' and CD as depicted in Figure 3B to assess the habit. These measurements are detailed in Table 1 and the Supplementary Material.

Statistical analyses. A correlation data matrix built with the six variables and 16 taxa, was prepared,

TABLE 2. Data of the three-dimensional scans.

3D scanned specimens	Equipment for data acquisition	Visualization	Volume reconstruction
Brontornis burmeisteri MLP-PV 20-570 *Phorusrhacos longissimus* MLP-PV 67-VIII-28-1	Kodak 9000 Extraoral Imaging System, using an exposition of 70 Kv 8mA 32.4s, a dose of 523 mGy.cm2, and a voxel size of 200µm x 200 µm x 200 µm.	Software CS 3D Imaging v3.5.18 (Carestream Health Inc)	InVesalius 3.1.
Patagornis marshi MLP-PV 20-85 and MLP-PV 20-86 *Psilopterus colzecus* MLP-PV 76–IV-12-2 *Andrewsornis abbotti* MLP-PV 59-II-26-83	X-Mind Trium manufactured by Gotzen Acteon Group, with CT of 110x80, and a thickness of 0.15.	Software AIS 3D app (UDI 08050038830010; Version 5.20210331).	Software AIS 3D app (UDI 08050038830010; Version 5.20210331).

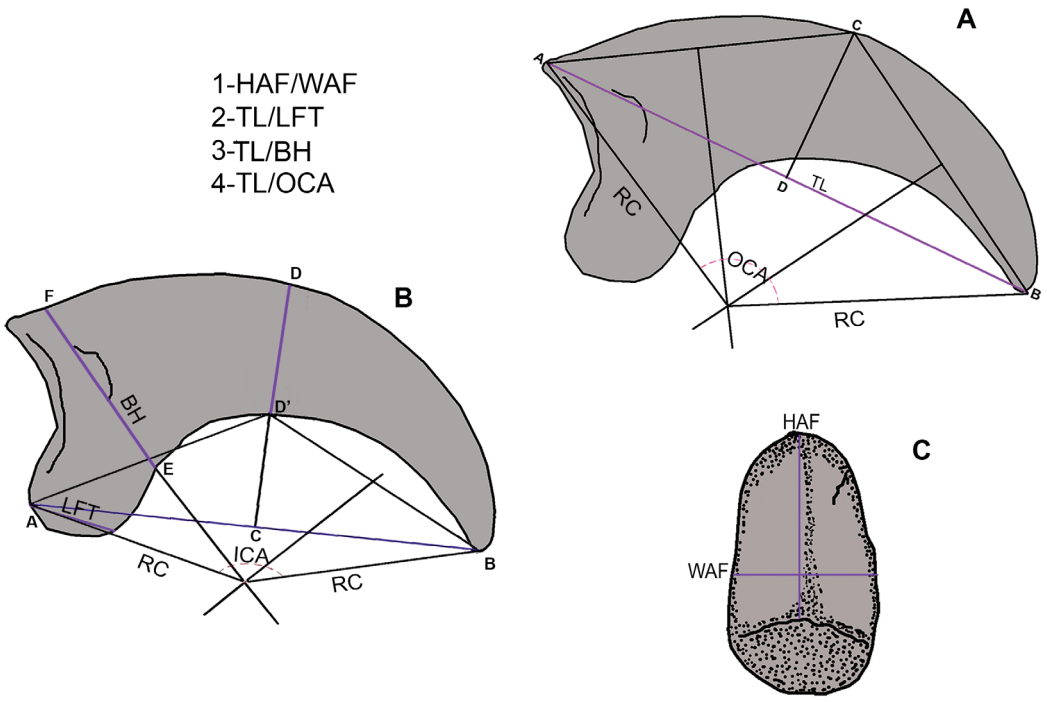

FIGURE 3. Linear and angular measurements taken on the schematic ungual phalanges in A-B lateral, and C, proximal views. Abbreviations: BH, basal height; HAF, maximum height of the articular facet; ICA, inner curvature angle; LFT, flexor tubercle length; OCA, outer curvature angle; TL, total length; and WAF, maximum width of articular facet.

and processed using the software PAST (Hammer, 2001). To reduce the number of variables in the dataset, while retaining as much information as possible, a Principal Component Analysis (PCA) was conducted (Sneath and Sokal, 1973) using a correlation matrix, taking into account the contribution of the individual variables to each component (Blackith and Reyment, 1971). The Jollife cut-off method was employed to identify and retain the significant principal components (Jolliffe, 2002). Prior to the PCA, linear correlation analyses were performed to evaluate the redundancy of variable information.

The selection of taxa for the PCA was based on the identification of MLP-PV 13-XI-28-546 (and presumably MLP-PV 14-I-10-199) as a ground-dwelling bird. Therefore, all modern birds included in the analysis were ground-living species, meaning birds that primarily spend a significant amount of time on the ground. We therefore included *Caracara plancus* (Falconiformes), *Vultur gryphus* (Catharthiformes), *Chauna torquata* (Anseriformes), *Apteryx australis* (Apterygiformes), *Dromaius novaehollandiae* (Struthioniformes), *Otis tarda* (Otidiformes), *Chunga burmeisteri* and *Cariama cristata* (Cariamiformes Cariamidae). The fossil specimens correspond to Phorusrhacidae with ungual phalanges certainly associated with taxonomically determined materials (*Procariama simplex* MACN 8275, *Phorusrhacos longissimus* AMNH 9497, *Psilopterus colzecus* MLP-PV 76 –IV-12-2, *Titanis walleri* UF 10417, *Paraphysornis brasiliensis* DGM-1418-R, *Andrewsornis abbotti* MLP-PV 59-II-2682-83, *Devincenzia pozzi* MACN Pv 6681), excluding all the other isolated phalanges used for descriptions and listed in Appendix 1.

Two separate analyses were conducted, each evaluating different aspects of the fossils within the context of the selected sample. In the first analysis, the five lineal variables listed above (TL, HAF, WAF, LFT, BH), plus the outer curvature angle (OCA), schematized in Figure 3A-C, were used in their absolute values. In the second analysis, the ratios of these variables were standardized by dividing each variable by its geometric sample mean following the method outlined by Baur and

Leuenberger (2011). The standardized ratios were then converted into indices to mitigate the influence of size variations in the results.

Systematics. The taxonomic assignment of the fossils was made following a thorough comparison with representatives of different orders of birds that exhibited at least one of the following features in their ungual phalanx: large size, high robustness, strong curvature, and hooked end. Additional comparisons were made with those groups of birds already documented in the Paleocene of Antarctica (Appendix 1). The taxonomical proposal concurs with Degrange et al. (2015) and Mayr (2016a) and adheres to the open nomenclatural recommendations of Bengtson (1988).

RESULTS

The results have been organized into different sections, each serving as specific purpose: Systematic paleontology (includes the description of the fossil MLP-PV 13-XI-28-546 and MLP-PV 14-I-10-199, anatomical identification of the materials, PCA with the linear and angular characters, higher?order taxonomic assignment comprising comparisons with representatives of the most relevant groups, and Intraordinal comparison with fossil and extant taxa.

SYSTEMATIC PALEONTOLOGY

Class Aves Linnaeus, 1758
Subclass Neognathae Pycraft, 1900
Order Cariamiformes Verheyen, 1957
?Phorusrhacidae Ameghino, 1889
Figure 4

Material 1. MLP-PV 13-XI-28-546 complete right ungual phalanx (Figure 4A, C, E, G, I).

Provenance. Fossil locality IAA 2/13, Seymour Island (Antarctic Peninsula, West Antarctica). Ypresian (early Eocene) Cucullaea I Allomember, La Meseta Formation.

Description. The specimen consists of a robust, laterally compressed, and curved ungual phalanx with a small dorsal fragment of the tip missing (Figure 4A). The neurovascular sulcus is present along the entire length of both lateral and medial surfaces, though it is slightly wider and deeper on the medial side (Figure 4E). This sulcus is situated closer to the plantar surface than to the dorsal margin and is proximally shallower and wider. On the medial side, the sulcus bifurcates in the proximal region, with the lower branch extending further proximally. As it approaches the tip, the sulcus becomes more dorsally positioned and is partially covered by a thin bony layer in certain areas. The claw becomes increasingly latero-medially compressed toward the tip (Figure 4C).

The articular surface exhibits a sub-triangular to ovoidal outline, with a main dorso-ventral axis (Figure 4G). The plantar side is rounded and approximately twice as wide as the dorsal margin, making the lateral and medial margins of the articular surface visible in dorsal view. The extensor tubercle is short and rounded, with minimal proximal projection. The articular surface is divided into two cotylae of similar size, slightly asymmetrical and dorsoventrally elongated. The lateral cotyla leans toward the lateral side, while the medial cotyla leans medially. Between them, the articular surface gently rises as a rounded ridge which is more pronounced in the area that contacts the flexor and extensor tubercles. The flexor tubercle is robust, rounded, and extends more toward the plantar and proximal directions than the extensor tubercle.

Material 2. MLP-PV 14-I-10-199 incomplete ungual phalanx (Figure 4B, DB, D, F, H).

Provenance. GPS S64°14’24.3’’, W56° 40’ 1.9’’, Seymour Island (West Antarctica). Cucullaea I Allomember, La Meseta Formation.

Description. The overall appearance of this specimen closely resembles MLP-PV 13-XI-28-546, although it is more fragmentary, and some features cannot be observed. The entire proximal face and dorsal surface are lacking, and the entire surface is covered with diagenetic cracks. Only the latero-medial and plantar facies of the phalanx body are preserved (Figure 4B, DB, D). As a result, it is not possible to obtain linear and angular measurements. The neurovascular sulcus is present on both sides, like in MLP-PV 13-XI-28-546 (Figure 4B, FB, F).

Anatomical identification. The ungual phalanges display characteristic morphologies for each digit with minor differences between families (Figure 5). The ungual of digit I is the smallest, relatively gracile, and weakly curved, and presents a long flexor tubercle. The ungual of digit II is highly curved, latero-medially compressed, dorsoventrally tall (with a sub-elliptic transverse section) and possesses a well-developed plantarly rounded flexor tubercle. The ungual of digit III is less curved and dorso-ventrally lower than digit II, with a short and plantarly flattened flexor tubercle (although it is caudally expanded in *Mesembriornis* and *Chunga burmeisteri* and develops lateral wings in *Brontornis burmeisteri*); consequently, it has a sub-triangular section. The ungual of digit IV is less curved and plantarly wider than those of digits II and III.

FIGURE 4. Fossil cariamiforms examined here. Ungual phalanx of the second right digit MLP-PV 13-XI-28-546 (A, C, E, G) in lateral (A), dorsal (C), medial (E), and proximal (G) views, and ungual phalanx of second digit MLP-PV 14-I-10-199 (B, D, F) in lateral or medial (B, F) and dorsal (D) views. Scale bar: 10 mm.

Given the latero-medial compression, sub-oval outline of the articular face, and strong curvature, MLP-PV 13-XI-28-546 and MLP-PV 14-I-10-199 are both assigned to the second digit. Additionally, the outline and asymmetry of the articular facets (medial and lateral cotylae), along with the slight curvature of the central axis of the corpus phalanx, indicate that MLP-PV 13-XI-28-546 belongs to the right foot. The incompleteness of MLP-PV 14-I-10-199 precludes a more precise identification.

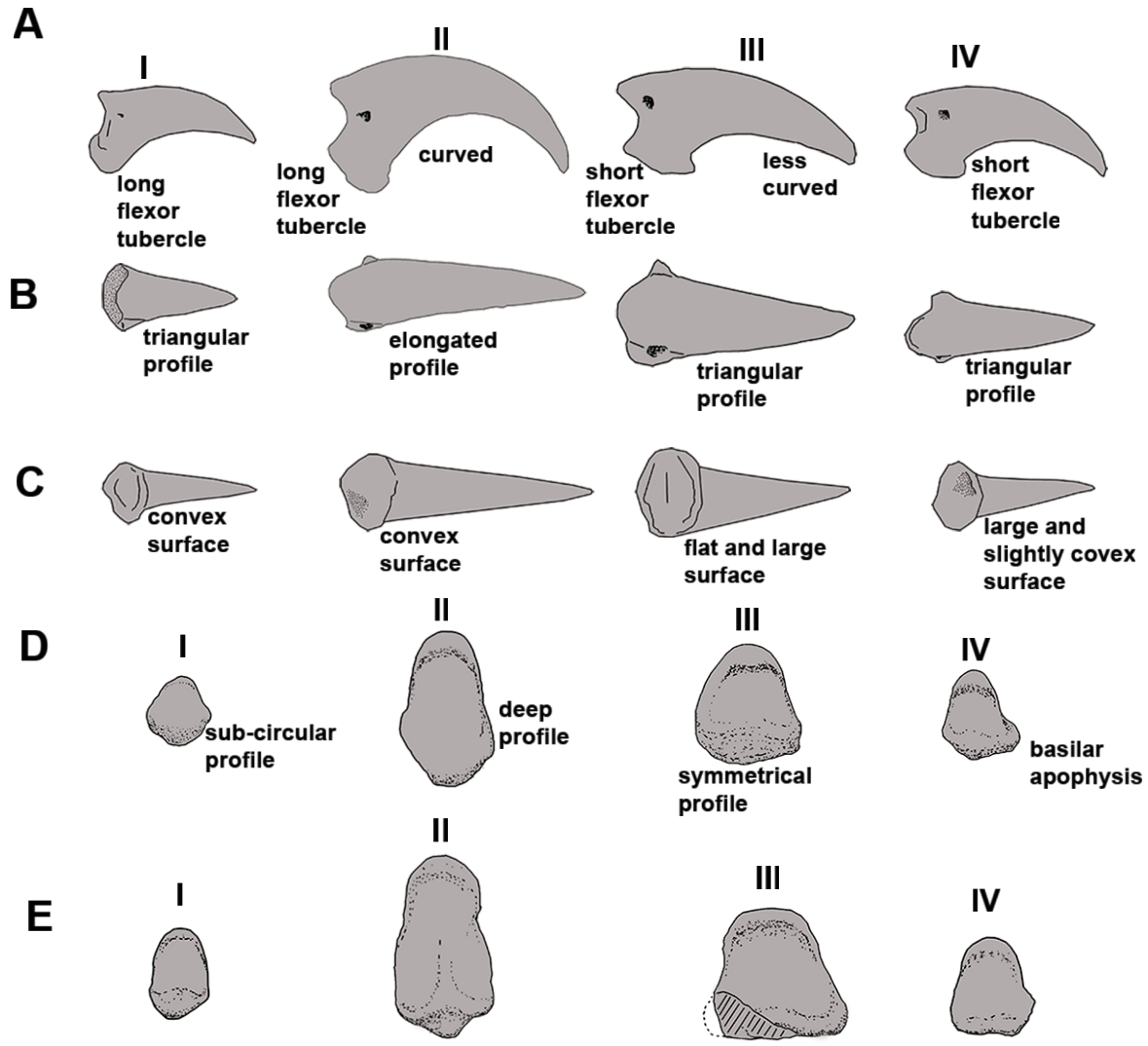

FIGURE 5. Morphological differences between the ungual phalanges of each digit (I, II, II, and IV) of *Cariama cristata* (A-D) and *Psilopterus colzecus* (E) in A, lateral; B, dorsal; C, plantar; D and E, proximal (articular) views (not scaled).

Principal Component Analysis. In the analysis of absolute values, most of the explained variation is concentrated in the first two components, with the first axis (PC1) explaining 81.73 % of the variation and the second axis (PC2) explaining 14.13%. Together, these two components account for 95.85% of the total variation (Appendix 2). Phorusrhacidae and Cariamidae form distinct groups in the analysis (Figure 6), with Phorusrhacidae mostly located in the upper right quadrant. MLP-PV 13-XI-28-546 is positioned close to *Phorusrhacos longissimus* presumably within Phorusrhacidae.

The first axis (PC1), which explains most of the variation, is primarily influenced by basal height (BH), followed by maximum width of the articular facet (WAF), total length (TL), and maximum height of the articular facet (HAF). Larger species like *Titanis* and *Devincenzia* have higher values in these variables. On the contrary, the flexor tubercle length (LFT), behaves differently. It decreases along the first axis (where it significantly loads) but increases along the second one (in which it has a negligible influence).

The larger *Titanis walleri* and *Devincenzia pozzi* occupy the extreme values on the first and second axis, whereas the smaller *Psilopterus colzecus* and *Procariama simplex* are at the other end of the Phorusrhacidae polygon.

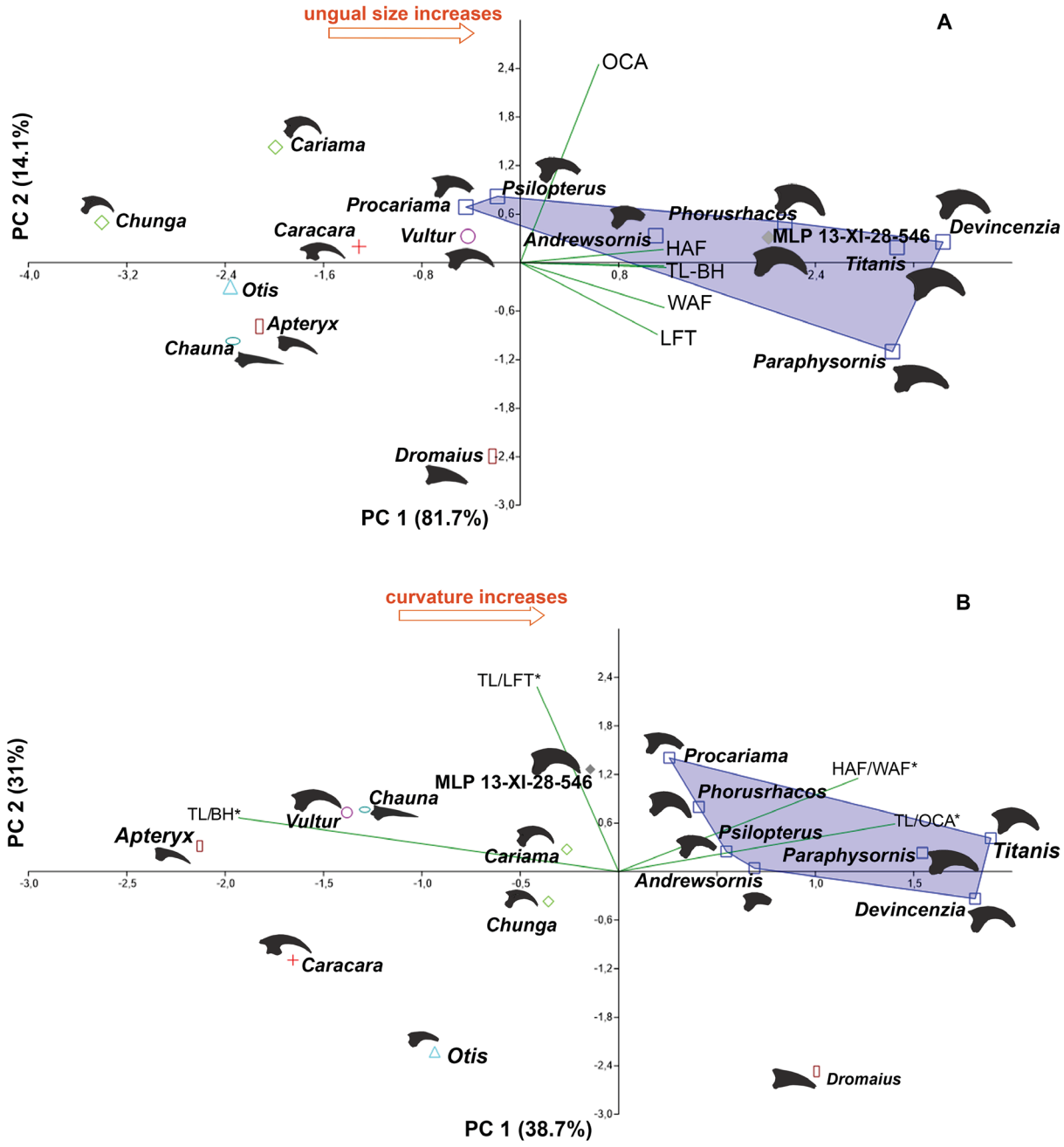

FIGURE 6. Biplot of the Principal Component Analyses (PCA). A, Analysis without normalization of data; B, Analysis with variables converted into indexes. Abbreviations: BH, basal height; HAF, maximum height of the articular facet; ICA, inner curvature angle; LFT, flexor tubercle length; OCA, outer curvature angle; TL, total length; and WAF, maximum width of articular facet.

Living Cariamidae are separated from Phorusrhacidae and other groups of birds and occupy the lower left quadrant. The raptorial Falconiformes *(Caracara plancus)* and Cathartiformes *(Vultur gryphus)* are in the upper left quadrant, whereas the more terrestrial Otidiformes *(Otis tarda,* formerly included within Gruiformes), Anseriformes *(Chauna torquata),* and ratites *(Apteryx australis* and *Dromaius novahollandiae),* are in the lower left area, distinct from Phorusrhacidae and Cariami-

dae. The morphology of *Dromaius* is rescued in this analysis, where it is far from the rest.

In the second analysis, in which the variables were converted into indexes to control the size influence, three components capture 91.95% of the accumulated explained variation (PC1 38.67%, PC2 30.49%, PC3 22.79%). The variables with the greatest weight in each component are total length/basal height (TL/BH) in PC1, total length/flexor tubercle length (TL/LFT) in PC2, and total length/outer angle (TL/OCA) in PC3.

When the first two axes are plotted, Phorusrhacidae and Cariamidae are once again distinguished as two separated groups, and MLP-PV 13-XI-28-546 falls in between them, definitively within the Cariamiformes cloud (Figure 6). Interestingly, MLP-PV 13-XI-28-546 is close to *Procariama simplex* and *Phorusrhacos longissimus*. Similar graphs are obtained when plotting PC3 against PC1 and PC2. Again, the representatives of other orders remain separated and from Cariamiformes (Cariamidae and Phorusrhacidae with MLP-PV 13-XI-28-546 included). In both analyses (absolute values and normalized data), Cariamiformes remain distinct from other robust (e.g., *Dromaius),* and predatory (e.g., *Caracara, Vultur)* forms.

Higher-order taxonomic assignment. MLP-PV 13-XI-28-546 (Figure 7A) and MLP-PV 14-I-10-199 are characterized by their large size and robusticity, strong curvature, and moderated projection of the flexor tubercle (only preserved in MLP-PV 13-XI-28-546). These features have not been observed in any previously recorded fossil bird in Antarctica, including Sphenisciformes, Procellariiformes, Anseriformes, Pelagornithidae, Gruiformes, Falconiformes, and flightless “Ratites”). Furthermore, these groups can be easily distinguished based on the following features.

Falconiformes (as well as Accipitriformes and Strigiformes) exhibit strongly curved and sharp claws, with a pronounced latero-medial compression, a conspicuous flexor tubercle oriented distally with two plantar foramina plantarly, and a large extensor tubercle (Figure 7D). Falconiformes are differentiated from Strigiformes (Figure 7F) by the presence of well-defined edges that delimit the ventral surface of the talon (as also described in Mosto and Tambussi, 2013).

On the opposite end extreme of spectrum, flightless Ratites (Figure 7G-I) and other large, ground-dwelling birds, typically present triangular, short, and flat phalanges. These phalanges are more elongated in Rheiformes (Figure 7I) and Struthioniformes (Figure 7H) and shorter in Dinornithiformes. However, in all cases, they maintain a large internal angle and are never curved plantarly. Lithonithiformes exhibit phalanges thar are moderately curved and slenderer (Nesbitt and Clarke, 2016: figs. 4, 10-12, 17, 19, 21). However, none of their phalanges closely resemble the condition observed in MLP-PV 13-XI-28-546 and MLP-PV 14-I-10-199. Other large and flightless birds worth comparing here are Gastornithiformes (Worthy et al. 2017). In Gastornithidae, the ungual phalanges are only slightly curved, while in Dromornithidae they are essentially flat and rounded.

Teratornithiformes and Cathartiformes also deserve attention due to their large to giant size. A single ungual phalanx (MMP s/n) from the Late Miocene Epecuén Formation (Buenos Aires Province, Argentina), was initially assigned to *Argentavis magnificens* (Campbell, 1995), but later reinterpreted as a phorusrhacid (Cenizo et al., 2012). Unfortunately, there are no other known phalanges of *Argentavis* or any other teratorn for direct comparisons. However, they have traditionally been considered morphologically similar to Cathartiformes in many aspects such as the proportions and anatomy of the limbs (e.g., Miller, 1909; Campbell, 1995). *Vultur gryphus* (Figure 7C) presents a relatively curved and sharp ungual phalanx, with greater latero-medial compression, and a flexor tubercle more ventrally expanded, rather than proximally. Other groups widely recorded in Antarctica, such as Sphenisciformes, Procellariiformes, Anseriformes, and Pelagornithidae, have ungual phalanges that are notably less curved (Figure 7O-Q). The ungual phalanges of giant penguins (Figure 7P) come closest in robustness and morphology to MLP-PV 13-XI-28-546 and MLP-PV14-I-10-199. These penguins have unguals that are dorsoventrally lower, less sharply hooked, and with a shorter and less developed flexor tubercle.

In contrast, the unguals of Procellariiformes, Anseriformes (Figure 7N), and Pelagornithidae (Howard, 1957: fig. 8) are thinner, more gracile, and notably less curved. Furthermore, with a single record, Gruiformes are also known to have existed in the Antarctic Eocene (Davies et al., 2020). Within Gruiformes, terrestrial psophids exhibit ungual phalanges barely curved, particularly considering the inner curvature. They have a rounded flexor tubercle more distally located than in the fossils studied here, which is completely separated from the articular facets. Other taxa previously considered gruiforms, such as Rhynochetidae, Eurgypygidae, and Aptornithidae, have slightly curved ungual corpus, and exposed neurovascular sulcus,

FIGURE 7. Ungual phalanx of representatives of the most relevant groups compared with the Antarctic specimens described in this study. A, Antarctic fossil MLP-PV 13-XI-28-546; B, *Chunga incerta* (Cariamiformes); C, *Vultur gryphus* (Cathartiformes); D, *Caracara plancus* (Falconiformes); E, *Geranoaetus melanoleucus* (Accipitriformes); F, *Ninox novaeseelandiae* (Strigiformes); G, *Casuarius casuarius* (Casuariformes); H, *Dromaius novaehollandiae* (Struthioniformes); I, *Rhea americana* (Rheiformes); J, *Tinamus solitarius* (Tinamiformes); K, *Penelope obscura* and L, *Crax fasciolata* (Galliformes); M, *Otis tarda* (Otidiformes); N, *Chauna torquata* (Anseriformes); O, *Macronectes giganteus* (Procellariiformes); P, *Anthropornis grandis* (giant Antartic Sphenisciformes); and Q, *Pygoscelis antarctica* (modern Sphenisciformes). Scale bar: 10 mm.

with a very short flexor tubercle that differs from the fossil material studied here (Parker, 1868; Worthy and Holdaway, 2002).

Finally, Cariamiformes (Figure 7B) also possess distinctive phalanges characterized by moderate latero-medial compression, strong internal and external curvature, and a flexor tubercle proximally and plantarly expanded, similar to MLP-PV 13-XI-28-546 and MLP-PV 14-I-10-199. Members of Phorusrhacidae and Cariamidae show even stronger curvatures and sharply hooked ungual phalanges, with these features more pronounced in digit II. In contrast, the phalanges of Idiornithidae (Mayr 2016b, fig. 1) and Bathornthidae (Mayr 2016a, fig. 9) are less curved and have a rounded and shorter flexor tubercle.

COMPARISONS WITH CARIAMIDAE AND PHORUSRHACIDAE

MLP-PV 13-XI-28-546 and MLP-PV 14-I-10-199 fall within a size range comparable to *Phorusrhacos longissimus* (MLP-PV 20-572, MLP-PV 67-VIII-28-1, and MLP-PV 20-139). Both, MLP-PV 13-XI-28-546 and MLP-PV 14-I-10-199, are larger

FIGURE 8. Antarctic ungual phalanx compared with different Phorusrhacidae species in lateral view. A, MLP-PV 13-XI-28-546; B, *Phorusrhacos longissimus* (AMNH 9497 taken from Sinclair and Farr 1932 and mirrored); C, *Procariama simplex* MACN 8275; D, *Phorusrhacus* (MLP-PV 20-572); E, *Paraphysornis brasiliensis;* F, *Patagornis marshi* MLP-PV 20-184; G, *Procariama simplex* MACN 8225; H, *Devincenzia pozzi* MACN Pv 6681; I, *Titanis walleri* (calcotype UF 10417); J, Psilopterinae indet. MLP-PV 90-III-5-56; K, *Mesembriornis milneedwardsi* MACN Pv 5944; L, *Patagornis marshi* MLP-PV 20-164; M, *Psilopterus colzecus* MLP-PV 76-VI-12-2; N, Psilopterinae indet. MPEF-PV 12256; O, MMP s/n Phorusrhacidae (re-drawn from Cenizo et al., 2012). Scales bar: 10 mm (except for C, G, M, and N where the scale represents 20 mm).

than *Psilopterus colzecus, Patagornis marshi,* and *Andrewsornis abbotti*, but smaller than *Devincenzia pozzi* (Figure 8).

The latero-medial compression of MLP-PV 13-XI-28-546 and MLP-PV 14-I-10-199 is less pronounced compared to *Psilopterus* but comparable to compression observed in *Phorusrhacos* and *Devincenzia*. This feature is closely related to the shape of the articular (proximal) surface. The articular surface is dorso-ventrally (=dorso-plantarly) lower than that of *Devincenzia, Ps. colzecus, Patagornis,* and *Procariama*, which have an ovoidal outline. MLP-PV 13-XI-28-546 instead approaches the condition observed in Phorusrhacidae MPEF-Pv 12156, and Psilopterinae MLP-PV 90-III-5-56, which have a wider plantar surface and a more sub-triangular outline.

From a qualitative point of view, the internal and external curvatures can differentiate hooked phalanges. Among Cariamiformes, the most pronounced curvature (or lower inner and outer curvature angles) is found in *Cariama cristata*, followed by *Chunga burmeisteri* and *Ps. colzecus*. Although phalanges MLP-PV 13-XI-28-546 and MLP-PV 14-

I-10-199 may appear as hooked as *Phororhacus*, based on t the preserved portions, they exhibit a more moderate curvature (see Table 1).

A parameter closely related to the inner and outer curvature is the robusticity index, which was calculated at 0.41. This value supports the inclusion of MLP-PV 13-XI-28-546 (and *Phorusrhacos longissimus*) within the category of ground and predatory birds.

In MLP-PV 13-XI-28-546, the flexor tubercle is elongated and rounded, although narrower and proximo-plantarly more projected than in other members of Cariamiformes. The flexor tubercle of MLP-PV 13-XI-28-546 is distally wider and more proximally projected, whereas it projects more plantarly in *Titanis*. In *Devincenzia* and *P. colzecus*, the flexor tubercle is wider and sturdier, and slightly more plantarly projected, while in *Brontornis* is also wider but shorter and less elongated. In *Procariama simplex*, the flexor tubercle is similarly elongated, but has a truncated tip. In extant Cariamidae, the flexor tubercle is elongated and plantarly pointing, slightly more rounded in *Cariama cristata* and sharp in *Chunga burmeisteri*. The flexor tubercle is shorter, and not elongated in *Patagornis*, and *Messembriornis*, and slightly bulkier towards the sides in MLP-PV 13-XI-28-546 and *Andrewsornis abbotti* (MLP-PV 59-II-26-83) than in other phorusrhacids and cariamids. It is plantarly flat in *Phorusrhacos longissimus* MLP-PV 67-VIII-28-1 and rounded in MLP-PV 20-572, *Cariama cristata*, *Psilopterus colzecus,* and *Devincenzia pozzi*. Unfortunately, these features cannot be objectively compared in MLP-PV 14-I-10-199 (Figure 8).

The extensor tubercle of MLP-PV 13-XI-28-546 is short and not proximally projected like in *Chunga burmeisteri* and *Cariama cristata* and *Procariama simplex* and *Psilopterus colzecus*. In *Phorusrhacos longissimus*, the extensor tubercle moderately projected, but definitively more than in MLP-PV 13-XI-28-546. In *Brontornis* the extensor tubercle is also proximally expanded, but more rounded and robust, delimiting dorsally the articular proximal facets. In a proximal view, the extensor tubercle coincides with separation of the medial and lateral cotylae. Elongation of the extensor tubercle of MLP-PV 13-XI-28-546 is less pronounced than in *Titanis* and resembles *Paraphysornis* and *Patagornis marshi.*

The neurovascular sulcus (Figure 9) is open and marked in MLP-PV 13-XI-28-546 and MLP-PV 14-I-10-199, a feature also observed in *Patagornis marshi* MLP-PV 20-164, but not in *Patagornis marshi* MLP-PV 20-184, where the sulcus is shallower and barely marked. In *Andrewsornis abbotti* MLP-PV 59-II-26-83 and *Brontornis burmeisteri* MLP-PV 20-570, the neurovascular sulcus is absent, probably due to weathering or development of an internal channel (not externally visible) rather than an open sulcus. In *Psilopterus colzecus*, the sulcus is not visible in digit II, but is present in digit III. This sulcus is proximally shallower in *Phorusrhacos longissimus* MLP-PV 67-VIII-28-1.

DISCUSSION

The anatomical and systematic identification of isolated ungual phalanges

While systematics relying on isolated elements are evidently less robust compared to those based on more complete skeletons, ungual phalanges have demonstrated their reliability in identifying groups with extreme modifications. Examples include xenarthrans among mammals (Patiño and Fariña, 2017), deinonychosaurs (Oswald et al., 2023), and terror birds (Jones, 2010).

Among the most obvious characters studied in avian ungual phalanges are the curvature degree, closely related to their habits, and the neurovascular sulcus. While curvature is typically assessed through measurement of inner and outer angle (Figure 3) or described qualitatively condition, our understanding of the development and variations of the neurovascular sulcus remains limited.

The neurovascular sulcus has been proposed in previous contributions as a useful taxonomic feature for distinguishing Phorusrhacidae and Cariamidae from the stem groups Cariamiformes (Idiornithidae and Bathornithidae). While this sulcus was coded as absent in Cariamidae and Phorusrhacidae, and this condition was identified as a synapomorphy of the crown-group Cariamidae + Phorusrhacidae (see Mayr, 2016a), we have observed inter-specific variation of this feature within these families (Figures 5, 8-9 and Table 3).

In fact, the sulcus neurovascularis can manifest as either a deep or shallow groove that covers all or part of the sides of the phalanx, and even occasionally as a closed or partially closed channel (not externally visible unless exposed due to weathering). Within modern cariamids, variation in neurovascular sulcus development is noticeable between *Chunga burmeisteri* (Figure 7B) and *Cariama cristata* (Figure 5), and even among specimens of the same species. Additionally, in *Chunga burmeisteri* MLP ORN 629, this sulcus displays differential development between the medial and lat-

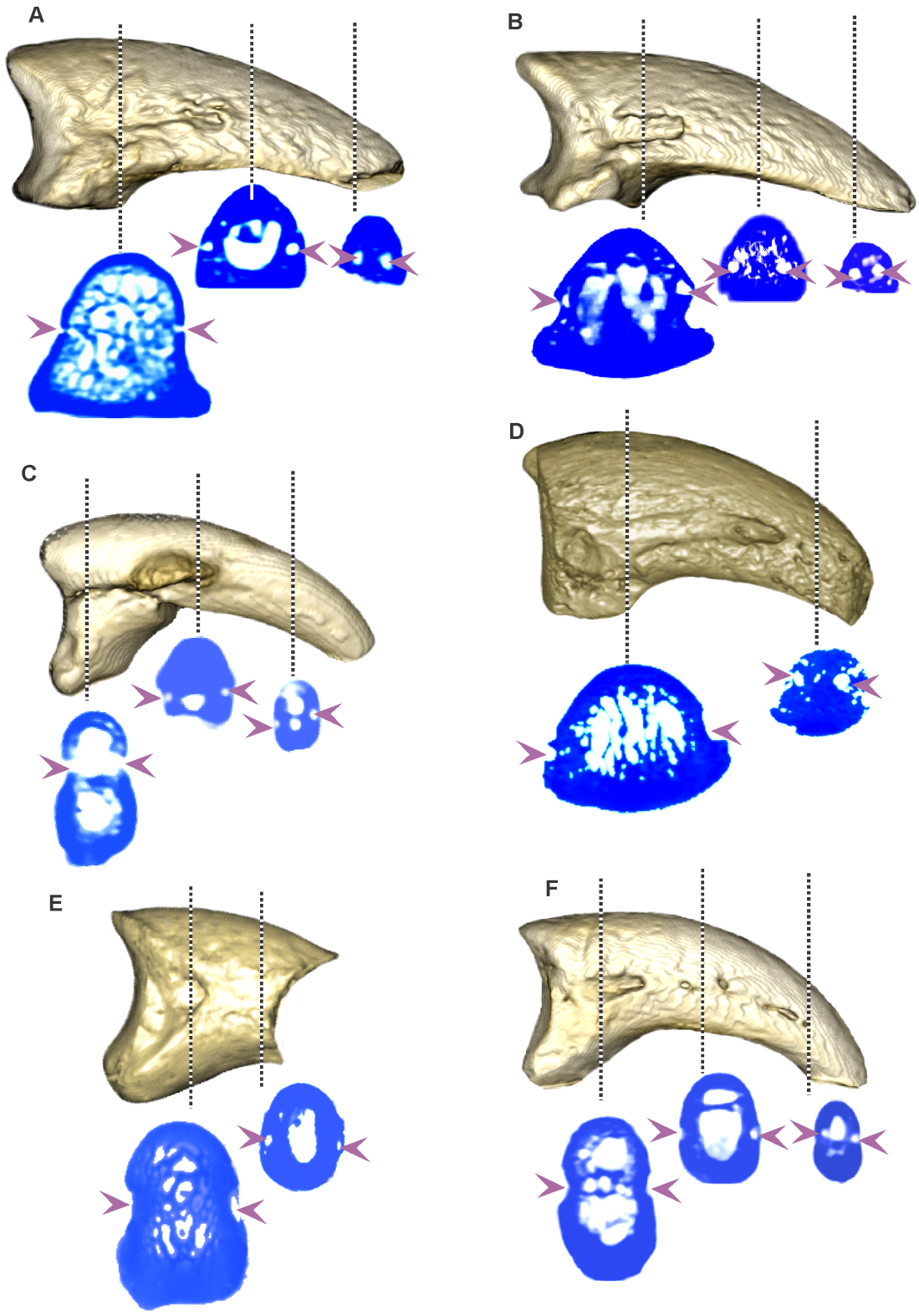

FIGURE 9. Three-dimensional reconstructions (not scaled) of different ungual phalanges. The dotted lines indicate the transversal cut areas shown below each phalanx. The arrowheads mark the path of the neurovascular sulcus and/or neurovascular canal along the phalanx. A, *Patagornis marshi* (MLP-PV 20-85, digit III); B, *Patagornis marshi* (MLP-PV 20-86, digit III); C, *Psilopterus colzecus* (MLP-PV 76-VI-12-2, digit II); D, *Brontornis burmeisteri* (MLP-PV 20-570, digit III); E, *Phorusrhacos longissimus* (MLP-PV 67-VIII-28-1, digit II); F, *Andrewsornis abbotti* MLP-PV 59-II-26-83 (digit II).

TABLE 3. Development of the neurovascular sulcus in different specimens of *Chunga burmeisteri* and *Cariama cristata*. Abbreviations: cs, complete sulcus; ps, partial sulcus; f, externally represented by a foramen; a, absent and presumably developed as an internal channel) in the left and right digits (I, II, III, IV), in the medial (M) and lateral (L) facies of the ungual phalanges.

Chunga burmeisteri MLP ORN 629	left digits							
	I (M)	I (L)	II (M)	II (L)	III (M)	III (L)	IV (M)	IV (L)
	f	f	f	a	ps	ps	ps	ps
	right digits							
	I (M)	I (L)	II (M)	II (L)	III (M)	III (L)	IV (M)	IV (L)
	a	f	f	f	ps	ps	ps	ps
Cariama cristata MNHN 5480	left digits							
	I (M)	I (L)	II (M)	II (L)	III (M)	III (L)	IV (M)	IV (L)
	f	f	f	f	f	f	f	f
	right digits							
	I (M)	I (L)	II (M)	II (L)	III (M)	III (L)	IV (M)	IV (L)
	f	f	f	f	f	f	f	f
Cariama cristata MNHN 6162	left digits							
	I (M)	I (L)	II (M)	II (L)	III (M)	III (L)	IV (M)	IV (L)
	f	f	f	f	f	f	f	f
	right digits							
	I (M)	I (L)	II (M)	II (L)	III (M)	III (L)	IV (M)	IV (L)
	f	f	f	f	f	f	f	f
Cariama cristata MNHN 8260	left digits							
	I (M)	I (L)	II (M)	II (L)	III (M)	III (L)	IV (M)	IV (L)
	f	f	f	f	f	f	f	f
	right digits							
	I (M)	I (L)	II (M)	II (L)	III (M)	III (L)	IV (M)	IV (L)
	f	f	f	f	f	f	f	f

eral sides of the same digit, as well as variation between the right and left foot (Table 3).

Among fossils, *Psilopterus colzecus* exhibits a partial sulcus on both sides of digit I, the lateral surface of digits III and IV, and a small foramen on both sides of digit II (Figures 8M, 9C), and the medial side of digits III and IV. On the other hand, the sulcus is open in *Mesembriornis milneedwardsi* (MACN-Pv 5944, digit II), with some areas covered with a thin bony layer, and in *Patagornis marshi* (Figure 9A-B), where it appears completely open (MLP-PV 20-164, digit II), or proximally covered by bone (MLP-PV 20-85 and MLP-PV 20-86, digits III). In *Devincenzia pozzi* (MACN Pv 6681, digit II) and *Brontornis* (MLP-PV 20-570, digit III), the sulcus is not externally visible, and only a proximal foramen indicates the presence of an internal channel (Figure 9D). The sulcus is almost completely exposed in *Phorusrhacos longissimus* (MLP-PV 20-139) and *Patagornis marshi* (MLP-PV 20-157, digit IV), without clear evidence of weathering. Therefore, the presence of an open sulcus could be interpreted as: (1) a taphonomic artifact from weathering; (2) incomplete ossification due to somatic immaturity; and (3) a condition variable in adult Cariamiformes, and present in many terror birds. For this reason, despite the use of sulcus neurovascularis form and development in current phylogenetic analyses (e.g., Smith, 2010; Mayr, 2021), the observed variations suggest caution in its use.

Implications for the evolution of body size of Caramiforms

The substantial sizes achieved by certain Phorusrhacidae species have attracted the attention of researchers more than once, leading to numerous attempts to estimate their size and body mass. Body size, particularly height, is possibly the more subjective of the two measures, as it relies on the reconstruction of body posture. Factors such as neck curvature, angular relationship between

the femur, tibiotarsus, and tarsometatarsus, and the relative spatial disposition of the pelvic girdle collectively determine overall height of the skeleton in life position (Degrange, 2012).

Calculating body mass can be achieved using various methods, each with different degrees of certainty. Early studies correlated body mass with body length the cross-sectional area of femur (Amadon, 1947). Subsequently, equations linking body mass to the minimum circumference of hindlimbs have been applied to flying teratorns, estimating up to 80 kg (Campbell and Tonni, 1983) and ratites estimating up to 81 kg (Anderson et al., 1985). Furthermore, by adopting a similar methodological approach and leveraging the minimum circumference of femurs or tibiotarsi in living birds, Campbell and Marcus (1992) introduced equations for estimating body mass, which rapidly became the most widely adopted methodology. In the case of Phorusrhacidae, two estimations were made, one based on comparisons with similar-sized modern birds (Alvarenga and Höfling, 2003) and the second using the Campbell and Marcus (1992) equations (Degrange, 2012; Degrange et al., 2012).

While ungual phalanges may not be ideal for body mass estimations, we use data from morphologically closer species as a proxy. The statistical analyses conducted in this study suggest that MLP-PV 13-XI-28-546 is morphologically more similar to *Phorusrhacos longissimus* than any other bird, including size. Both MLP-PV 13-XI-28-546 and *Phorusrhacos longissimus* have a robusticity index of 0.41, a value shared with *Paraphysornis brasiliensis* and *Andrewsornis abbotti*. This value suggests these species were ground and predatory birds, according to the polygons of Birn-Jeffery et al. (2012, fig. 3C-D). These findings support the idea that *P. longissimus*, known from a partially associated skeleton, serves as a reliable proxy for MLP-PV 13-XI-28-546 and for MLP-PV 14-I-10-199.

Previous estimations for *P. longissimus* AMNH 9497 have ranged from 117 kg (based on femur circumference; Degrange, 2012) to 130 kg (using size of homologous bones in a male ostrich; Alvarenga and Höfling, 2003). Even higher estimations of approximately 134 kg were obtained for *P. longissimus* MPM-Pv 4241 (Degrange et al., 2012). According to that, MLP-PV 13-XI-28-546 can be interpreted as a large, heavy ground bird with a body mass exceeding 100 kg.

It has been suggested that large body masses have were independently reached in different lineages around the early Miocene (Degrange et al., 2015) and possibly the late Oligocene (see *Physornis fortis* record in Degrange et al., 2015, figure 10). However, the discovery of MLP-PV 13-XI-28-546 and MLP-PV 14-I-10-199 in the early Eocene provides evidence that large sizes appeared earlier than previously thought, at least in Antarctica. This finding aligns with some paleoecological proposals. According to observations in extant species, it has been hypothesized that a bimodal distribution of body sizes is the norm for homeotherms living in extremely low temperatures (see Case, 2006). Small species would survive hostile conditions by consuming a high percentage of their body weight in food to reduce their metabolism during hibernation. In contrast, large homeotherms would retain heat during winter, due to their small surface/volume ratio. Either of these adaptive strategies would be inadequate for intermediate body sizes (Case, 2006) such as those of the oldest South American phorusrhacids. However, in recent years, a wide range of sizes has been reported for mammals from the La Meseta Formation in Antarctica (Gelfo et al., 2019), suggesting that a taphonomic bias may account for the scarcity of forms of intermediate size.

This is significant because body mass is a parameter closely related to the prey size in predatory vertebrates (Wheelwright, 1985), such as Phorusrhacidae, groups widely recognized as zoophagous (Worthy et al., 2017) and predators (Ameghino, 1895; Andrews, 1899; Alvarenga and Höfling, 2003; Blanco and Jones, 2005; Bertelli et al., 2007; Degrange, 2012; Jones, 2010; Tambussi et al., 2012).

The robusticity index calculated for the Antarctic materials and most representative phorusrhacid specimens places them within the polygon of ground and predatory birds. Specifically, the Antarctic specimen, *Phorusrhacos longissimus, Paraphysornis brasiliensis,* and *Andrewsornis abbotti* share the same value for this parameter, suggesting similar ecological roles. Birds similar in size to MLP-PV 13-XI-28-546 would have been capable of preying on similarly sized prey, approximately up to 100 kg. Despite discussions of their potential scavenging behavior, various independently calculated parameters such as bite force, the robusticity index, and running speed, in combination with size and body mass, strongly indicate their role as active predators that primarily fed on medium to large prey (Blanco and Jones, 2005; Degrange, 2012, 2015).

On the contrary, the moderate curvature of these phalanges approaching the condition of *Paraphysornis*, may also be associated with scavenging behaviors (see Alvarenga, 1993). Hypercarnivorous birds, like *Phorusrhacos*, typically develop a strongly curved ungual phalanx in the second digit to capture prey during hunting. This characteristic is also observed in Cariamidae and Psiloterinae, the most basal Phorusrhacidae (Jones, 2010).

Contributions to the reconstruction of the Antarctic communities of the Eocene

Although the La Meseta Formation is a marine unit deposited in a prodeltaic, deltaic, and mainly estuarine environment influenced by tides (Montes et al., 2019), the Cucullaea I Allomember is a fossiliferous layer with the most significant continental influence within the sequence. As a result, Cucullaea I represents the best stratigraphic level for gaining insight into the composition and structure of the terrestrial community. This level is associated with some of the most iconic localities (e.g., DPV 6/84, IAA 1/90, IAA 2/95, IAA 2/84, and IAA 2/16) that have yielded numerous land mammals and flying birds (Acosta Hospitaleche et al., 2019; Gelfo et al., 2019 for more details). Herbivorous groups dominated the community of land mammals and were represented by ungulates of various sizes with dental adaptations for feeding on different types of plants, folivorous xenarthrans, frugivorous gondwanatherians, and marsupials (Gelfo et al., 2019). The diversity of marsupials included small species with diverse dietary habits, including insectivores, frugivores, and folivores. Notably, there were no carnivores among continental mammals known for these levels, nor in the rest of Antarctica. In contrast, in other contemporary associations, such as those of Southern Patagonia (Argentina), the role of active hunters was fulfilled by large metatherians, such as the Sparassodonta (Gelfo et al., 2019).

Indirect evidence of predators among mammals comes from the middle Eocene Fossil Hill Formation exposed in Fildes Peninsula, South Shetland Islands (Mansilla et al., 2012b). A single isolated footprint (T-373) is characterized by the presence of a metapodial bilobate pad with subcircular digital pads and the absence of claw marks along its distal margin (Mansilla et al., 2012b). This finding could potentially mark the first evidence of mammalian predators. The footprint shares similarities with the ichnogenus *Felipeda* (Mansilla et al., 2012b), and may belong to a medium-sized metatherian (Gelfo, personal commun., 2023). Even though some of these forms could potentially be found at the Cucullaea I levels, the representation of top predators in the Eocene of Antarctica remains relatively under-represented.

Among birds, when excluding marine fauna, *Antarctoboenus carlinii* would be the only continental predator. *Antarctobaenus* is a medium-sized member of Falconiformes, initially classified as an indeterminate member of Polyborinae (Noriega and Tambussi, 1996), but more recently re-interpreted as a basal form (Cenizo et al., 2016). Large birds with hunting skills, like MLP-PV 13-XI-28-546 and MLP-PV 14-I-10-199, are well-suited for this ecological context, fitting the profile of apex predators. Furthermore, from the Fossil Hill Formation in the South Shetland Islands, certain avian tracks were identified, including morphotype I attributed to cursorial birds (Covacevich and Lamperein, 1969, 1970, 1972; Covacevich and Rich, 1982; Li and Zhen, 1994). The specific bird responsible for these tracks remains uncertain but the ichnological assemblage indicates a high diversity of middle Eocene birds.

The Eocene assemblages found in Antarctica differ significantly from modern communities. However, contemporaneous localities in Patagonia (Argentina) provide a partially valid comparative framework for analyzing the structure and dynamics of the Eocene Antarctic faunas. The faunal affinities between the Antarctic Peninsula and Southern South America have been attributed to the presence of continental connections, such as the early Paleogene Weddellian Isthmus (Reguero et al., 2014). The vertebrate assemblage of the La Meseta Formation is taxonomically similar to the coeval and slightly younger Eocene Patagonian fauna of Argentina located in Southern South America. Notable examples include the middle Eocene Vacan and the middle late Eocene Mustersan assemblages, where some of the earliest Phorusrhacidae-like birds were discovered. These assemblages reflect a “greenhouse” dominated by marsupials, xenarthrans, and ungulates, among mammals, elements that remind the La Meseta Formation composition (e.g., Bond and Deschamps, 2010; Goin et al., 2010). In these cases, land mammal communities were characterized by browsers (Ortiz-Jaureguizar and Cladera, 2006), with the role of top predators being fulfilled by mid-sized marsupials and large carnivorous birds.

During the Eocene, the representation of phorusrhacid-like birds was relatively low, and it was not until the Miocene that a significant diversifica-

tion of this group was observed. However, Cariamiformes, and possibly Phorusrhacidae, were already present in South America, as indicated by least a few records. Notably, there is some controversy in the identification of these early records. For instance, the early Eocene *Paleopsilopterus itaboraiensis* from Brazil has been interpreted as a member of Psilopterinae (Alvarenga, 1985; Alvarenga and Höfling, 2003; Degrange and Tambussi, 2011), Idiornithidae (Agnolín, 2009; Tambussi et al., 2023), or an indeterminate family within Cariamiformes (Degrange, 2010). Similarly, remains from the late Eocene of Gran Hondonada in Argentina have been assigned to Psilopterinae (Acosta Hospitaleche and Tambussi, 2005; Tambussi et al., 2023), Idiornithidae (Agnolín, 2009), or an uncertain Cariamiformes (Degrange, 2012). In addition, a widely accepted Phorusrhacidae from the middle Eocene of Cañadón Vaca, Argentina, was originally classified as a member of Psilopterinae (Tonni and Tambussi, 1986, 1988) but later simply mentioned as a phorusrhacid (Tambussi et al., 2023). The lack of consensus in identifying these remains may be attributed to the incomplete nature of the fossils and the ongoing challenge of determining distinctive features for Cariamiformes families.

MLP-PV 13-XI-28-546 and MLP-PV 14-I-10-199, from the Antarctic Cucullaea I Allomember, come from levels slightly older than the earliest known Patagonian Phorusrhacidae from the middle Eocene (Tonni and Tambussi, 1986, 1988). Beyond the intra-ordinal assignment, the presence of *Paleopsilopterus itaboraiensis* (Alvarenga, 1985) and the fossils from Gran Hondonada (Acosta Hospitaleche and Tambussi, 2005) confirm the presence of Cariamiformes in South America and Antarctica since the early Eocene.

CONCLUSIONS

All the Antarctic materials previously assigned to Phorusrhacidae have been reclassified into other bird lineages, reflecting the significant advancements in our understanding of the Antarctic fossil avifauna over the last decades. In other cases, like the avian ichnites, the assignment remains uncertain. SizeThe size and morphology of these footprints are consistent with the expected for phorusrhacids smaller than MLP-PV 13-XI-28-546 and MLP-PV 14-I-10-199, reflecting the bimodal pattern of sizes proposed by Case (2006) for Antarctic communities. The ungual phalanges described in this contribution provide limited but crucial information, and their systematic identity is beyond doubt. Furthermore, when considering multiple variables such as size and proportion, robustness, latero-medial compression, morphology, and development of the flexor and extensor tubercles, these findings offer insights into various paleobiological aspects, including body mass and habit. What makes these discoveries unique is not just their systematic identity but also the extraordinary size of the specimens, the geographic location, and the age of the carrier sediments.

After qualitative comparisons and quantitative analyses, we concluded that MLP-PV 13-XI-28-546 falls within Cariamiformes. However, differences in results reflect data treatment. When measurements are analyzed without normalization, MLP-PV 13-XI-28-546 is grouped within Phorusrhacidae. Yet, when variables are transformed into indexes to control the effect of the size, MLP-PV 13-XI-28-546 is located in a morphospace between Cariamidae and Phorusrhacidae. In summary, MLP-PV 13-XI-28-546 (and probably also MLP-PV 14-I-10-199) belongs to Cariamiformes and may be included in the crown-group Cariamidae-Phorusrhacidae, probably within Phorusrhacidae. However, the information derived from the ungual phalanges is limited, suggesting caution in the intra-ordinal allocation. The Antarctic specimens MLP-PV 13-XI-28-546 and MLP-PV 14-I-10-199 likely belong to large/giant predators -possibly also scavengers, similar in size to *Phorusrhacos longissimus* size. They most likely preyed on small- and medium-sized vertebrates (Figure 10). These birds would be active hunters that fulfilled the role of continental apex predators apparently sub-occupied by mammals in the Paleogene Antarctic communities. Large Phorusrhacidae-like birds represent a guild hitherto unknown to Antarctica. These findings unequivocally reshape our understanding of the dynamic of early Eocene Antarctic continental ecosystems.

ACKNOWLEDGEMENTS

We thank the Dirección Nacional del Antártico and the Instituto Antártico Argentina for the invitation to field, and to Fuerza Aérea Argentina for logistic support. J.N. Gelfo, D. García López, and F. Irazoqui invaluably collaborated in field and P. Carreiras kindly made the tomographies assisted by Dr. J.N. Gelfo. Partial help was provided by the Consejo Nacional de Investigaciones Científicas y Tecnológicas (PIP 0096), Universidad Nacional de La Plata (N955 and N953), and Agencia Nacional de Promoción Científica y Tecnológica (PICT 2017 0607). Lic. M. Charnelli drew the paleoenvironmen-

FIGURE 10. Paleoenvironmental reconstruction of the Ypresian continental communities of Seymour Island. A large Cariamiform hunting a medium-sized ungulate and staring at *Notiolofos reguerοi* (Mammalia: Sparnotheriodontidae), a couple of marsupials on a tree, *Antarctoboenus carlinii* (Aves, Falconiformes) flying on the sky, and a flightless Ratites in the back.

tal reconstruction. Finally, we thank the editors and two anonymous reviewers for their comments.

Author contributions. Conceptualization C Acosta Hospitaleche (CAH) and W Jones (WJ); Material curation CAH and WJ; Data acquisition CAH and WJ; Statistical Analysis WJ; Three-dimensional reconstructions CAH; Funding Acquisition CAH and WJ; Investigation CAH and WJ; Methodology CAH and WJ; Validation CAH and WJ; Writing – Original Draft Preparation – Review and Editing - Preparation of figures CAH and WJ.

REFERENCES

Acosta Hospitaleche, C., Jadwiszczak, P., and Clarke, J.A. 2019. The fossil record of birds from the James Ross Basin, West Antarctica. Advances in Polar Sciences, 30:251–273. https://doi.org/10.13679/j.advps.2019.0014

Acosta Hospitaleche, C., Reguero, M.A., and Santillana, S. 2017. *Aprosdokitos mikrotero* gen. et sp. nov., the tiniest Sphenisciformes that lived in Antarctica during the Paleogene. Neues Jahrbuch für Geologie und Paläontologie-Abhandlungen, 283:25–34. https://doi.org/10.1127/njgpa/2017/0624

Acosta Hospitaleche, C., and Tambussi, C.P. 2005. Phorusrhacidae Psilopterinae (Aves) en la Formación Sarmiento de la localidad de Gran Hondonada (Eoceno Superior), Patagonia, Argentina. Spanish Journal of Palaeontology, 20:127–132. https://doi.org/10.7203/sjp.20.2.20551

Agnolin, F.L. 2009. Sistemática y Filogenia de las Aves Fororracoideas (Gruiformes: Cariamae). Monografías Fundación Azara, Buenos Aires, Argentina.

Agnolin, F.L. 2021. Reappraisal on the phylogenetic relationships of the enigmatic flightless bird *(Brontornis burmeisteri)* Moreno and Mercerat, 1891. Diversity, 13:1–90. https://doi.org/10.3390/d13020090

Alvarenga, H.M.F. 1985. Um novo Psilopteridae (Aves: Gruiformes) dos sedimentos terciarios de Itaborai, Rio de Janeiro, Brasil", Congresso Brasileiro de Paleontologia, NME-DNPM, Rio de Janeiro, pp. 17–20.

Alvarenga, H.M.F. 1993. *Paraphysornis* novo gênero para *Physornis brasiliensis* Alvarenga, 1982 (Aves: Phorusrhacidae). Anais da Academia Brasileira de Ciências, 65:403–406.

Alvarenga, H.M.F., Chiappe, L.M., and Bertelli, S. 2011. The terror birds; pp. 187–208. In Dyke, G. and Kaiser, G. (eds.), Living Dinosaurs: The Evolutionary History of Modern Birds. Wiley-Blackwell, Chichester, U.K.

Alvarenga, H.M., and Höfling, E. 2003. Systematic revision of the Phorusrhacidae (Aves: Ralliformes). Papéis Avulsos de Zoologia, 43:55–91. https://doi.org/10.1590/s0031-10492003000400001

Amadon, D. 1947. An estimated weight of the largest known bird. The Condor, 49:159–164. https://doi.org/10.2307/1364110

Ameghino, F. 1895. Sobre las aves fósiles de Patagonia. Boletín del Instituto Geográfico de Argentina, 15:501–602.

Anderson, J.F., Hall-Martin, A., and Russell, D.A. 1985. Long-bone circumference and weight in mammals, birds and dinosaurs. Journal of Zoology, 207:53–61. https://doi.org/10.1111/j.1469-7998.1985.tb04915.x

Andrews, C. 1899. On the extinct birds of Patagonia, I, the Skull and skeleton of *Phororhacos inflatus* Ameghino. Transactions of the Zoological Society of London, 15:55–86. https://doi.org/10.1111/j.1096-3642.1899.tb00019.x

Angst, D. and Buffetaut, É. 2017. Palaeobiology of giant flightless birds. Elsevier. https://doi.org/10.1016/c2015-0-06179-2

Angst, D., Buffetaut, E., Lécuyer, C., and Amiot, R. 2013. "Terror Birds" (Phorusrhacidae) from the Eocene of Europe imply trans-Tethys dispersal. PLoS ONE, 8:e80357. https://doi.org/10.1371/journal.pone.0080357

Baumel, J.J., King, A.S., Breazile, J.E., Evans, H.E., and Vanden Berge, J.C. 1993. Handbook of Avian Anatomy: Nomina Anatomica Avium, 2nd Edition. Nuttall Ornithological Club, Cambridge, Massachusetts.

Baur, H. and Leuenberger, C. 2011. Analysis of ratios in multivariate morphometry. Systematic Biology, 60:813–825. https://doi.org/10.1093/sysbio/syr061

Bengtson, P. 1988. Open nomenclature. Palaeontology, 31:223–227.

Bertelli, S., Chiappe, L.M., and Tambussi, C.P. 2007. A new phorusrhacid (Aves, Cariamae) from the middle Miocene of Patagonia, Argentina. Journal of Vertebrate Paleontology, 27:409–19. https://doi.org/10.1671/0272-4634(2007)27[409:anpacf]2.0.co;2

Birn-Jeffery, A.V., Miller, C.E., Naish, D., Rayfield, E.J., and Hone, D.W. 2012. Pedal claw curvature in birds, lizards, and Mesozoic dinosaurs–complicated categories and compensating for mass-specific and phylogenetic control. PLoS ONE, 7:e50555. https://doi.org/10.1371/journal.pone.0050555

Blackith, R.E. and Reyment, R.A. 1971. Multivariate morphometrics. Academic Press, London, UK.

Blanco, R.E. and Jones, W.W. 2005. Terror birds on the run: a mechanical model to estimate its maximum running speed. Proceedings of the Royal Society B: Biological Sciences, 272:1769–1773. https://doi.org/10.1098/rspb.2005.3133

Bond, M. and Deschamps, C.M. 2010. 17 The Mustersan age at Gran Barranca: a review. The paleontology of Gran Barranca: evolution and environmental change through the Middle Cenozoic of Patagonia, 255–263

Brodkorb, P. 1963. A giant flightless bird from the Pleistocene of Florida. Auk, 80:111–115. https://doi.org/10.2307/4082556

Brodkorb, P. 1967. Catalogue of fossil birds: part 3 (Ralliformes, Ichthyornithiformes, Charadriiformes). University of Florida. https://doi.org/10.2307/4511456

Buffetaut, E. and Angst, D. 2021. *Macrornis tanaupus* Seeley, 1866: an enigmatic giant bird from the upper Eocene of England. Geological Magazine, 158:1129–1134. https://doi.org/10.1017/s0016756820001466

Campbell, Jr., K.E. 1995. Additional specimens of the giant teratorn, *Argentavis magnificens,* from Argentina (Aves: Teratornithidae). Courier Forschungsinstitut Senckenberg, 181:199–201. https://doi.org/10.5962/p.208145

Campbell, K.E. and Marcus, L. 1992. The relationship of hindlimb bone dimensions to body weight in birds. In Campbell, K.E. (ed.), Papers in Avian Paleontology honoring Pierce Brodkorb. Natural History Museum Los Angeles County, Science Series 36, 395412.

Campbell, K.E. and Tonni, E.P. 1983. Size and locomotion in Teratorns (Aves Teratornithidae). The Auk, 100:390–403. https://doi.org/10.1093/auk/100.2.390

Case, J.A. 2006. The late Middle Eocene terrestrial vertebrate fauna from Seymour Island: the tails of the Eocene Patagonian size distribution. Geological Society, London, Special Publications, 258:177–186. https://doi.org/10.1144/gsl.sp.2006.258.01.13

Case., J.A., Woodburne, M., and Chaney, D. 1987. A gigantic phororhacoid (?) bird from Antarctica. Journal of Paleontology, 61:1280–1284. https://doi.org/10.1017/s0022336000029681

Case, J.A., Reguero, M., Martin, J., and Cordes-Person, A. 2006. A cursorial bird from the Maastrichtian of Antarctica. Journal of Vertebrate Paleontology, 26, 48A.

Cenizo, M.M. 2012. Review of the putative Phorusrhacidae from the Cretaceous and Paleogene of Antarctica: new records of ratites and pelagornithid birds. Polish Polar Research, 3:239–258. https://doi.org/10.2478/v10183-012-0014-3

Cenizo, M.M., Tambussi, C.P., and Montalvo, C.I. 2012. Late Miocene continental birds from the Cerro Azul Formation in the Pampean region (central-southern Argentina). Alcheringa: An Australasian Journal of Palaeontology, 36:47–68. https://doi.org/10.1080/03115518.2011.582806

Cenizo, M., Noriega, J.I., and Reguero, M.A. 2016. A stem falconid bird from the Lower Eocene of Antarctica and the early southern radiation of the falcons. Journal of Ornithology, 157:885–894. https://doi.org/10.1007/s10336-015-1316-0 https://doi.org/10.1007/s10336-015-1316-0

Chávez, M. 2007. Fossil birds of Chile and Antarctic Peninsula. Arquivos do Museu Nacional, Rio de Janeiro, 65:551–572.

Covacevich, V. and Lamperein, C. 1969. Nota sobre el hallazgo de icnitas fósiles de aves en Península Fildes, Isla Rey Jorge, Shetlands del Sur, Antártica. Instituto Antártico Chileno Boletín, 4:26–28.

Covacevich, V. and Lamperein, C. 1970. Hallazgo de icnitas en Penıínsula Fildes, Isla Rey Jorge, archipiélago Shetlands del Sur, Antártica. Serie Científica del Instituto Antártico Chileno, 1:55–74.

Covacevich, V. and Lamperein, C. 1972. Ichnites from Fildes Peninsula, King George Island, South Shetland islands. In Adie, J.A., ed. Antarctic geology and geophysics. Oslo: Universitetsforlaget, 71–74.

Covacevich, V. and Rich, P.V. 1982. New birds ichnites from Fildes Peninsula, King George Island, West Antarctica, pp. 245–254. In Craddock, C. (ed.), Antarctic Geoscience. Wisconsin University Press, Madison.

Cracraft, J. 1968. A review of the Bathornithidae (Aves, Gruiformes), with remarks on the relationships of the suborder Cariamae. American Museum Novitates, 2326:1–46.

Cracraft, J. 1971. Systematics and evolution of the Gruiformes (Class Aves) 2. Additional comments on the Bathornithidae, with descriptions of new species. American Museum Novitates, 2449:1–14.

Davis, S.N., Torres, C.R., Musser, G.M., Proffitt, J.V., Crouch, N.M., Lundelius, E.L., Lamanna, M., and Clarke, J. 2020. New mammalian and avian records from the late Eocene La Meseta and Submeseta formations of Seymour Island, Antarctica. PeerJ, 8:e8268. https://doi.org/10.7717/peerj.8268

Degrange, F.J. 2012. Morfología del cráneo y complejo apendicular posterior de aves fororracoideas: implicancias en la dieta y modo de vida. Doctoral dissertation, Universidad Nacional de La Plata.

Degrange, F. 2015. Hind limb morphometry of terror birds (Aves, Cariamiformes, Phorusrhacidae): Functional implications for substrate preferences and locomotor lifestyle. Earth and Environmental Science Transactions of The Royal Society of Edinburgh, 106:257–276.

Degrange, F.J. and Tambussi, C.P. 2011. Re-examination of Psilopterus lemoinei (Moreno and Mercerat, 1891), a late early Miocene little terror bird from Patagonia (Argentina). Journal of Vertebrate Paleontology, 31:1080–1092. https://doi.org/10.1080/02724634.2011.595466

Degrange, F.J., Tambussi, C.P., Taglioretti, M., Dondas, A., and Scaglia, F. 2015. A new Mesembriornithinae (Aves, Phorusrhacidae) provides new insights into the phylogeny and sensory capabilities of terror birds. Journal of Vertebrate Paleontology, 35:e912656. https://doi.org/10.1080/02724634.2014.912656

Dunn, R.E., Strömberg, C.A.E., Madden, R.H., Kohn, M.J., and Carlini, A.A. 2015. Linked canopy, climate, and faunal change in the Cenozoic of Patagonia. Science, 347:258–261. https://doi.org/10.1126/science.1260947

Feduccia, A. 1993. Evidence from claw geometry indicating arboreal habits of *Archaeopteryx*. Science, 259:790–793. https://doi.org/10.1126/science.259.5096.790

Gelfo, J.N., Goin, F.J., Bauzá, N., and Reguero, M. 2019. The fossil record of Antarctic land mammals: commented review and hypotheses for future research. Advances in Polar Sciences, 30:274–292. https://doi.org/10.13679/j.advps.2019.0021

Goin, F.J., Abello, M.A., and Chornogubsky, L. 2010. Middle Tertiary marsupials from central Patagonia (early Oligocene of Gran Barranca): understanding South America's Grande Coupure. The paleontology of Gran Barranca: evolution and environmental change through the Middle Cenozoic of Patagonia, 7:69–105.

Gonzaga, L.P. 1996. Family Cariamidae (Seriemas), pp. 234–239. In del Hoyo, J., Elliot, A., and Sargatal, J. (eds.), Handbook of Birds of the World Vol. III.

Hammer, O. 2001. PAST: Paleontological statistics software package for education and data analysis. Palaeontología Electrónica, 4:1–9. https://palaeo-electronica.org/2001_1/past/issue1_01.htm

Howard, H. 1957. A gigantic 'toothed' marine bird from the Miocene of California. Santa Barbara Museum of Natural History Department of Geology Bulletin, 1:1–23.

Jolliffe, I.T. 2002. Principal Component Analysis, (2nd edition) Springer-Verlag, New York. Springer-Verlag, New York.

Jones, W. 2010. Nuevos aportes sobre la paleobiología de los fororrácidos (aves: phorusrhacidae) basados en el análisis de estructuras biológicas. Doctoral Dissertation, PEDECIBA-Universidad de la República.

Jones, W., Rinderknecht, A., Alvarenga, H., Montenegro, F., and Ubilla, M. 2018. The last terror birds (Aves, Phorusrhacidae): New evidence from the late Pleistocene of Uruguay. Paläontologische Zeitschrift, 92:365–372. https://doi.org/10.1007/s12542-017-0388-y

Kramarz, A.G., Bond, M., and Carlini, A.A. 2019. Astrapotheres from Cañadón Vaca, Middle Eocene of central Patagonia: new insights on diversity, anatomy, and early evolution of Astrapotheria. Palaeontologia Electronica, 22.2.52A:1–22. https://doi.org/10.26879/986

Li, J. and Zhen, S. 1994. New materials of bird ichnites from Fildes Peninsula, King George Island of Antarctica, and their biogeographic significance, pp. 239–250. In Shen Yanbin (ed.), Stratigraphy and Palaeontology of Fildes Peninsula, King George Island, Antarctica. Science Press, Beijing.

Mansilla, H.G., De Valais, S., Stinnesbeck, W., Varela, N.A.Y., and Leppe, M.A. 2012a. New Avian tracks from the lower to middle Eocene at Fossil Hill, King George Island, Antarctica. Cambridge University Press; Antarctic Science, 24:500–506. https://doi.org/10.1017/s0954102012000260

Mansilla, H., De Valais, S., Frey, E., Leppe, M., Varela, N., and Stinnesbeck, W. 2012b. Huella de mamíferos del Eoceno, Isla Rey Jorge, Antártica. In 3° Simposio de Paleontología en Chile.

Marenssi, S., Santillana, S., and Rinaldi, C. 1998. Stratigraphy of La Meseta Formation (Eocene), Marambio Island, Antarctica, pp. 137–146. In Casadío, S. (ed.), Paleógeno de América Del Sur y de La Península Antártica, Revista de la Asociación Paleontológica Argentina.

Mayr, G. 2016a. Osteology and phylogenetic affinities of the middle Eocene North American *Bathornis grallator*—one of the best represented, albeit least known Paleogene cariamiform birds (seriemas and allies). Journal of Paleontology, 90:357–374. https://doi.org/10.1017/jpa.2016.45

Mayr, G. 2016b. Avian feet, crocodilian food and the diversity of larger birds in the early Eocene of Messel. Palaeobiodiversity and Palaeoenvironments, 96:601–609. https://doi.org/10.1007/s12549-016-0243-2

Mayr, G. 2021. A partial skeleton of a new species of *Tynskya* Mayr, 2000 (Aves, Messelasturidae) from the London Clay highlights the osteological distinctness of a poorly known early Eocene “owl/parrot mosaic”. Paläontologische Zeitschrift, 95:337–357. https://doi.org/10.1007/s12542-020-00541-8

Mayr, G. 2022. Paleogene Avifaunas: A Synopsis of General Biogeographic and Paleoecological Aspects, p. 227–239. In: Paleogene Fossil Birds, Springer, Cham. https://doi.org/10.1007/978-3-030-87645-6_11

Mcfadden, B., Labs-Hochstein, J., Hulbert, R.C., Jr., and Baskin, J.A. 2007. Revised age of the late Neogene terror bird *(Titanis)* in North America during the Great American Interchange. Geology, 35:123–126. https://doi.org/10.1130/g23186a.1

Miller L. 1909. *Teratornis* a new avian genus from Rancho La Brea. Bulletin of the Department of Geology University of California Publications, 5:305–317. https://doi.org/10.2307/1362021

Montes, M. Martín, F.N., Santillana, S., Marenssi, S., Olivero, E.B., and González, A.M. 2008a. Mapa geológico 1: 20.000 de la Isla Marambio (mar de Weddell, Antártida). Geotemas, 10:709–712.

Montes, M., Nozal, F., Santillana, S., Marenssi, S., and Olivero, E. 2013. Mapa Geológico de isla Marambio (Seymour); escala 1:20.000. Serie Cartográfica Geocientífica Antártica. Con texto complementario. Madrid-Instituto Geológico y Minero de España; Buenos Aires-Instituto Antártico Argentino.

Montes, M., Santillana, S., Martín, F.N., and Marenssi, S. 2008b. El Paleoceno superior de la Antártida: la Formación Cross Valley-Wiman de la isla Marambio (mar de Weddell). Geotemas, 10:665–668.

Montes, M., Nozal, F., Olivero, E., Gallastegui, G., Santillana, S., Maestro, A., López-Martínez, J., González, L., and Martín-Serrano, A. 2019. Geología y Geomorfología de isla Marambio (Seymour). In Montes, M.F.N. and Santillana, S. (eds.), Madrid-Instituto Geológico y Minero de España; Buenos Aires-Instituto Antártico Argentino, Madrid.

Moreno, F.P. and Mercerat, A. 1891. Catálogo de los pájaros fósiles de la República Argentina conservados en el Museo de La Plata. Anales del Museo de La Plata, 1:7–71.

Mosto, C. and Tambussi, C. 2014. Qualitative and quantitative analysis of talons of diurnal bird of prey. Anatomia, Histologia, Embryologia, 43:6–15. https://doi.org/10.1111/ahe.12041

Mourer-Chauviré, C. 1983. Les Gruiformes (Aves) des Phosphorites du Quercy (France). I. Sous-order Cariamae (Cariamidae et Phorusrhacidae) systématique et biostratigraphie. Paleovertebrata, 13:83–143.

Mourer-Chauviré, C., Tabuce, R., Mahboubi, M.H., Adaci, M., and Bensalah, M. 2011. A Phororhacoid bird from the Eocene of Africa. Naturwissenschaften, 98:815–823. https://doi.org/10.1007/s00114-011-0829-5

Nesbitt, S.J. and Clarke, J.A. 2016. The anatomy and taxonomy of the exquisitely preserved Green River formation (early Eocene) Lithornithids (Aves) and the relationships of Lithornithidae. Bulletin of the American Museum of Natural History, 406:1–91. https://doi.org/10.1206/0003-0090-406.1.1

Noriega, J.I. and Mayr, G. 2017. The systematic affinities of the putative seriema *Noriegavis santacrucensis* (Noriega et al., 2009) from the Miocene of Argentina. Contribuciones del MACN, 7:133–139.

Noriega, J. and Tambussi, C. 1996. The non penguin avifauna from the Eocene (early Oligocene?) of Seymour Island, Antarctic Peninsula. Fourth International Meeting of the Society of Avian Paleontology and evolution. Abstracts: 13, Washington.

Ortiz-Jaureguizar, E. and Cladera, G.A. 2006 Paleoenvironmental evolution of southern South America during the Cenozoic. Journal of Arid Environments, 66:498–532. https://doi.org/10.1016/j.jaridenv.2006.01.007

Oswald, T., Curtice, B., Bolander, M., and Lopez, C. 2023. Observation of Claw Use and Feeding Behavior of the Red-Legged Seriema and Its Implication for Claw Use in Deinonychosaurs. Journal of the Arizona-Nevada Academy of Science, 50:17–21. https://doi.org/10.2181/036.050.0103

Palópolo, E.E., Brezina, S.S., Casadio, S., Griffin, M., and Santillana, S. 2021. A new zoroasterid asteroid from the Eocene of Seymour Island, Antarctica. Acta Palaeontologica Polonica, 66:301–318. https://doi.org/10.4202/app.00714.2019

Parker, W.K. 1868. XVII. On the Osteology of the Kagu *(Rhinochetus jubatus).* The Transactions of the Zoological Society of London, 6:501–522.

Patiño, S.J. and Fariña, R.A. 2017. Ungual phalanges analysis in Pleistocene ground sloths (Xenarthra, Folivora). Historical Biology, 29:1065–1075. https://doi.org/10.1080/08912963.2017.1286653

Pike, A.V.L., and Maitland, D.P. 2004. Scaling of bird claws. Journal of Zoology, 262:73–81. https://doi.org/10.1017/s0952836903004382

Reguero, M.A., Gelfo, J.N., López, G.M., Bond, M., Abello, A., Santillana, S.N., and Marenssi, S.A. 2014. Final Gondwana breakup: the Paleogene South American native ungulates and the demise of the South America–Antarctica land connection. Global and Planetary change, 123:400–413. https://doi.org/10.1016/j.gloplacha.2014.07.016

Rinaldi, C.A., Massabie, A., Morelli, J., Rosenman, H.L., and Del Valle, R. 1978. Geologia de la isla Vicecomodoro Marambio. Contribución del Instituto Antártico Argentino, 217:1–37.

Smith N.D. 2010. Phylogenetic analysis of Pelecaniformes (Aves) based on osteological data: implications for waterbird phylogeny and fossil calibration studies. PloS ONE, 5:e13354. https://doi.org/10.1371/journal.pone.0013354

Sneath, P.H.A. and R.E. Sokal. 1973. Numerical Taxonomy. W. H. Freeman Co., San Francisco, California.

Soto-Acuña, S., Bostelmann, E., Buldrini, K.E., Otero, R.A., and Oyarzún, J. L. 2014. First record of a fossil seriema (Cariamiformes: Cariamidae) from Chile. IV Simposio Paleontología en Chile, Universidad Austral de Chile, Valdivia, p. 88

Tambussi, C. and Acosta Hospitaleche, C. 2007. Antarctic birds (Neornithes) during the Cretaceous-Eocene times. Revista de la Asociación Geológica Argentina, 62:604–617.

Tambussi, C.P. Degrange, F. 2013. The Paleogene birds of South America. South American and Antarctic continental Cenozoic birds: paleobiogeographic affinities and disparities, 29–47. https://doi.org/10.1007/978-94-007-5467-6_5

Tambussi, C.P., Degrange, F.J., and De Mendoza, R.S. 2023. "The current state of knowledge of the Cenozoic birds of Argentina" by Tonni 1980: Four Decades After. Publicación Electrónica de la Asociación Paleontológica Argentina, 23:255–295. https://doi.org/10.5710/peapa.13.08.2022.418

Tambussi, C.P., De Mendoza, R., Degrange, F.J., and Picasso, M.B. 2012. Flexibility along the neck of the Neogene terror bird I (Aves, Phorusrhacidae). PLoS ONE, 7:e37701. https://doi.org/10.1371/journal.pone.0037701

Tambussi, C.P., and Noriega, J.I. 1996. Summary of the avian fossil record from southern South America. Münchner Geowissenschaftliche Abhandlungen, 30:245–264.

Tonni, E.P. 1974. Un nuevo cariamido (Aves, Gruiformes) del Plioceno superior de la provincia de Buenos Aires. Ameghiniana, 11:366–372.

Tonni, E.P. and Tambussi, C.P. 1986. Las aves del Cenozoico de la República Argentina. Quinto Congreso Argentino de Paleontología y Estratigrafía, Actas, 2:131–142.
Tonni, E.P. and Tambussi, C.P. 1988. Un nuevo Psilopterinae (Aves: Ralliformes) del Mioceno tardío de la provincia de Buenos Aires, República Argentina. Ameghiniana, 25:155–160.
West, A.R., Torres, C.R., Case, J.A., Clarke, J.A., O'Connor, P.M., and Lamanna, M.C. 2019. An avian femur from the Late Cretaceous of Vega Island, Antarctic Peninsula: removing the record of cursorial landbirds from the Mesozoic of Antarctica. PeerJ, 7:e7231. https://doi.org/10.7717/peerj.7231
Wheelwright, N.T. 1985. Fruit size, gape width, and the diet of fruit-eating birds. Ecology, 66:808–818. https://doi.org/10.2307/1940542
Winkler, D.W., Billerman, S.M., and Lovette, I.J. 2020. Seriemas (Cariamidae), version 1.0. In Birds of the World (Billerman, S. Keeney, B., Rodewald, P., and Schulenberg, T. (eds.), Cornell Lab of Ornithology, Ithaca, NY, USA. https://doi.org/10.2173/bow.cariam1.01
Woodburne, M.O., and Zinsmeister, W.J. 1984. The first land mammal from Antarctica and its biogeographic implications. Journal of Paleontology, 58:913-948.
Worthy, T.H., Degrange, F.J., Handley, W.D., and Lee, M.S. 2017. The evolution of giant flightless birds and novel phylogenetic relationships for extinct fowl (Aves, Galloanseres). Royal Society Open Science, 4:170975. https://doi.org/10.1098/rsos.170975
Worthy, T.H., and Holdaway, R.N. 2002. The lost world of the moa: prehistoric life of New Zealand. Indiana University Press. https://doi.org/10.2307/4090128
Zinsmeister, W.J. 1982. Late Cretaceous and Tertiary aporrhaid gastropods from the southern rim of the Pacific Ocean. Journal of Paleontology, 56:84–102. https://doi.org/10.1017/s0022336000035216

APPENDIX 1

Comparative material.

Fossil specimens

Patagornis marshi: MLP-PV 20-157 (ungual phalanx digit IV), MLP-PV 20-164 (ungual phalanx of digit II in Degrange, 2012, and not included in Jones, 2010; however, following the criteria of Jones, 2010, it is assigned here to digit II), MLP-PV 20-85 (ungual phalanx of digit III concurring with Jones, 2010, not assigned to any digit in Degrange, 2012), MLP-PV 20-86 (ungual phalanx of digit III, not examined in Jones, 2010 and assigned to digit II in Degrange, 2012), MLP-PV 20-184 (ungual phalanx of digit II).

Andrewsornis abbotti: MLP-PV 59-II-26-83 (ungueal phalanx of digit II, not assigned to any digit in Degrange, 2012).

Phorusrhacos longissimus: MLP-PV 20-139 (digit III, only as ungual phalanx in Degrange 2012,), MLP-PV 67-VIII-28-1 (digit II) MLP-PV 67-VIII-28-2 (digit III)

Phorusrhacos: MLP-PV 20-572 (ungual pahalanx digit II).

Brontornis burmeisteri: MLP-PV 20-570 (ungual phalanx of digit III).

Psilopterus colzecus: MLP-PV 76-VI-12-2 (ungual phalanx of digits I-IV)

Psilopterinae: MLP-PV 90-III-5-56 (ungual phalanx of digit II), MLP-PV 90-III-5-57 (ungual phalanx of digits III)

Phorusrhacidae: MUSM 351 (ungual phalanx of digit III, taken from Shockey et al., 2009: fig. 4A), MLP-PV 59-II-24-228 (incomplete ungual phalanx), MLP-PV 73-VII-2-10 (badly preserved ungueal phalanx), MLP-PV s/n (field Number 95-159).

Titanis walleri calcotype MNHN s/n (UF 10417)

Extant specimens (ungual phalanges of digit II)

Apteryx haasti: CMC-Av23661

Caracara plancus: MNHN 6390, MNHN 6391

Chunga burmeisteri: MLP ORN 629

Cariama cristata: MNHN 5480, MNHN 6162, MNHN 8260

Casuarius casuarius: MNHT 1813, MACN 53568

Chauna torquata: MNHN 5934, MNHN 5807

Crax fasciolata: MNHT 727

Dromaius novaehollandiae: MHNT 1870

Geranoaetus melanoleucus: MLP ORN 14371

Macronectes giganteus: MNHN 5804, MNHN 5479, MNHN 5804

Otis tarda: MHNT 79

Rhea americana: MLP ORN 1411, MLP ORN 1414, MNHN 6238

Penelope obscura: MHNT 202, MNHN 5669

Tinamus solitarius: MHNT 479, MNHN 6290

Vultur gryphus: MLP ORN 357, MACN 54749

APPENDIX 2

Linear correlation analysis and PCA outputs.

Correlation table for 5 variables. Below the main diagonal are linear correlation coefficients. Upright are the no correlation probability (significant no correlation <0.05. Yellow highlights indicate significant probability of no correlation)

Variable	TL	OCA	LFT	BH	HAF	WAF
TL	0	0.058487	8.52E-06	6.88E-09	1.55E-06	8.50E-08
OCA	0.46746	0	0.20969	0.12486	0.069843	0.25179
LFT	0.86229	0.32055	0	8.11E-06	3.06E-05	1.41E-07
BH	0.94851	0.38701	0.86324	0	1.60E-07	2.01E-08
HAF	0.89153	0.4501	0.83484	0.92081	0	7.21E-08
WAF	0.92741	0.29415	0.92221	0.94039	0.92902	0

PCA outputs for 6 variables. Jollife cut-off method for significant PC. Yellow highlights indicate a significant PC.

Correlation matrix	Jollife cut-off: 0.7	
PC	Eigenvalue	% variance
1	4.90356	81.726
2	0.848006	14.133
3	0.11525	1.9209
4	0.0764382	1.274
5	0.0346568	0.57761
6	0.0220869	0.36812

PCA loadings for 6 variables.

Loadings	Axis 1	Axis 2
TL	0.9675	-0.01365
OCA	0.5281	0.845
LFT	0.9243	-0.3058
BH	0.9813	-0.01997
HAF	0.9645	0.05665
WAF	0.97	-0.1913

Correlation table for 4 variables. Below the main diagonal (linear correlation coefficients). Upright the no correlation probability (significant correlation <0.05. Yellow highlights indicate significant probability of no correlation).

Variable	HAF/WAF*	TL/OCA*	TL/LFT*	TL/BH*
HAF/WAF*	0	0.7679	0.49299	0.21782
TL/OCA*	0.080164	0	0.64454	0.15355
TL/LFT*	0.1849	0.12503	0	0.21987
TL/BH*	-0.32603	-0.37401	0.32466	0

PCA outputs for 4 variables. Jollife cut-off method for significant PC. Yellow highlights indicate a significant PC.

PCA 4 variables correlation matrix		
Correlation matrix	**Jollife cut-off: 0.7**	
PC	**Eigenvalue**	**% variance**
1	1.54699	38.675
2	1.21982	30.495
3	0.911681	22.792
4	0.321511	8.0378

PCA loadings for 4 variables.

Loadings	Axis 1	Axis 2	Axis 3
HAF/WAF*	0.5582	0.4696	-0.645
TL/OCA*	0.6441	0.2403	0.6891
TL/LFT*	-0.1898	0.9318	0.1278
TL/BH*	-0.8858	0.2709	0.0672

SUPPLEMENTARY MATERIAL

Measurements taken on the materials.
Available for download at:
https://palaeo-electronica.org/content/2024/5019-eocene-cariamiformes-from-antarctica